NASA Contractor Report 191435

DEPARTMENT OF CHEMISTRY AND BIOCHEMISTRY
COLLEGE OF SCIENCES
OLD DOMINION UNIVERSITY
NORFOLK, VIRGINIA 23529

INSTRUMENTATION FOR HYPERSONIC AERODYNAMICS RESEARCH WITH TETHERED SATELLITES

By

Leonard T. Melfi, Jr.

and

Kenneth G. Brown, Jr., Principal Investigator

Final Report
For the period January 1, 1990 to January 15, 1992

Prepared for
National Aeronautics and Space Administration
Langley Research Center
Hampton, Virginia 23665

Under
Master Contract NAS1-18584
Task Authorization No. 73
Kenneth H. Crumbly, Technical Monitor
PROJ-Projects Development Branch

January 1992

DEPARTMENT OF CHEMISTRY AND BIOCHEMISTRY
COLLEGE OF SCIENCES
OLD DOMINION UNIVERSITY
NORFOLK, VIRGINIA 23529

INSTRUMENTATION FOR HYPERSONIC AERODYNAMICS RESEARCH WITH TETHERED SATELLITES

By

Leonard T. Melfi, Jr.

and

Kenneth G. Brown, Jr., Principal Investigator

Final Report
For the period January 1, 1990 to January 15, 1992

Prepared for
National Aeronautics and Space Administration
Langley Research Center
Hampton, Virginia 23665

Under
Master Contract NAS1-18584
Task Authorization No. 73
Kenneth H. Crumbly, Technical Monitor
PROJ-Projects Development Branch

Submitted by the
Old Dominion University Research Foundation
P.O. Box 6369
Norfolk, Virginia 23508-0369

January 1992

TABLE OF CONTENTS

ACRONYMS

A/D	Analog to Digital
BCU	Bench Checkout Unit
CPU	Central Processing Unit
FED	Flight Electronics Division, NASA, LaRC
FIFO	First In First Out
GSFC	Goddard Space Flight Center, NASA
GTOSS	Generalized Tethered Orbiting Satellite Simulation
IBM®	International Business Machines®
IRD	Instrument Research Division, NASA, LaRC
LaRC	Langley Research Center, NASA
MSFC	Marshall Space Flight Center, NASA
NASA	National Aeronautics and Space Administration
PC	Personal Computer
SED	System Engineering Division, NASA, LaRC
SEDS	Small Expendable Deployer System
TN	Technical Note, NASA

LIST OF TABLES

LIST OF FIGURES

SUMMARY

This report describes the work accomplished under Contract Number NAS1-18584 entitled " *Master Agreement for Research in the Physical and Life Sciences,* " Task 73 entitled " *Instrumentation for Hypersonic Aerodynamics Research with Tethered Satellites* " with NASA, LaRC. The work began on January 2, 1990 and extended through December 31, 1991. The first year's effort concentrated on Shuttle borne tether satellite systems, measurement requirements, instrumentation assessment, aerothermodynamic instrumentation definition, and tether technology. These aspects were studied in detail and are reported in a review article entitled " *Downward Deployed Tethered Satellite Systems, Measurement Techniques, and Instrumentation: A Review* " by Kenneth G. Brown, Jr. et. al. which has been accepted for publication in the May/June 1992 issue of the **Journal of Spacecraft and Rockets** (See Part II). The second year's effort concentrated on the development of computer codes to analyze instrument data from NASA's SEDS mission. This mission is planned to fly in early 1993 and consists of an instrumented end-mass deployed with a tether from an orbiting second stage of a Delta rocket. The objective of this mission (from the tethered end-mass point of view) is to determine end-mass dynamics, i.e. spatial position and orientation as a function of flight time. The end-mass contains a 3-axis load cell, a 3-axis accelerometer, and a 3-axis magnetometer. Part I of this report describes the computer conversion of instrument output data to engineering units and the display of this data in convenient form to allow end-mass dynamics to be studied.

STATEMENT OF WORK*

INSTRUMENTATION FOR HYPERSONIC AERODYNAMICS RESEARCH WITH TETHERED SATELLITES

Scope of Project - Since 1984, NASA has conducted definition studies to deploy an instrumented satellite from the Space Shuttle on a 100 km long tether to allow rarefied aerothermodynamic data to be obtained in the atmosphere at altitudes as low as 110 km. During 1990, preliminary data requirements for this mission have been defined and consist of the following: freestream gas composition and density; surface pressure; surface temperature; heat flux rates; position, altitude, and velocity; acceleration; attitude and rotation; tether vector at the satellite; and tether tension at the satellite. In 1991, it is planned to define required measurements, instrumentation, and technology developments necessary to study aerodynamic effects on tethered satellites.

Scope of the Work - There are 7 subtasks which are considered within the scope of work on this task. They are as follows:

1. Detailed definition of the previously identified data and measurement requirements.

2. Assessment of the current state of the art of instrumentation and identification of necessary instrument technology development.

* This statement of Work has been modified slightly to include present knowledge of NASA's plans

3. Definition of instrumentation necessary to conduct the planned rarefied aerothermodynamics experiments.

4. Identify aspects of tether technology which may significantly reduce the cost and risk of space transportation operations.

5. Develop computer codes and/or spreadsheet models to convert SEDS-1 satellite data files into engineering-units time histories. Calibration and temperature compensation functions will be implemented and tested with simulated data in a format specified in the GSFC Data Quality Assurance Plan.

6. Identify/derive an analytical description of SEDS-1 satellite orientation and rotation rates as a function of vector acceleration, tether tension, and magnetic field measurements, assuming given directions of the local magnetic field and tether relative to the satellite.

7. Implement algorithms developed under subtask 6 into computer codes and test with simulated mission dynamics data.

Comments - The work outlined in subtask 1 through 4 was accomplished during the first year of this two year effort and was concerned mainly with Shuttle borne tether systems, measurement requirements, instrumentation assessment, aerothermodynamic instrumentation definition, and tether technology. A review article entitled " *Downward Deployed Tethered Satellite Systems, Measurement Techniques, and Instrumentation: A Review* " by Kenneth G. Brown, Jr. et. al. which has been accepted for publication in the May/June 1992 issue of the **Journal of**

Spacecraft and Rockets is attached to this report as Part II. This article details the work accomplished in the first four subtasks shown above and no further discussion of the work accomplished under these subtasks will be included here. This report will concentrate on SEDS end-mass instrument data analysis undertaken in the second year of this work. Due to NASA imposed limitations on time and resources, work during the second year concentrated on subtask 5. It was planned to continue the work on subtask 6 and 7, after completing subtask 5, as a continuing effort during 1992. The preliminary work accomplished under subtask 6 and 7, such as the implementation of the GTOSS 4-D display program, is not ready to report at this time. The next section of this report gives a brief review of the SEDS mission followed by detailed accomplishments on subtask 5.

SEDS END-MASS MISSION

An instrumented end-mass payload will be deployed from the orbiting second stage of a Delta rocket using a small diameter tether 20 km in length (See Fig. 1.). At about 90 minutes after deployment, the tether is cut and the end-mass and tether re-enters the atmosphere. The objective of the end-mass portion of this mission is to determine the dynamics of a payload at the end of a long tether in Earth orbit. The development of the deployer mechanism and tether, and the dynamic analysis of the second stage Delta and tether (including tether length measurements) are managed by MSFC and are not a part of the data analysis discussed in this report. The end-mass being fabricated and instrumented by LaRC is a rectangular box consisting of: sensors and electronics mounted on a baseplate; a deployment and attachment mechanism for attaching the end-mass to the second stage of the Delta rocket and deploying the end-mass; and an isolation mechanism to minimize vibration during deployment. Mounted on the baseplate are three sensor systems, a 3-axis load cell, a 3-axis accelerometer, and a 3-axis magnetometer. The load cell measures tether tension at the end-mass and this three axis data can be used to determine tether angle with respect to the

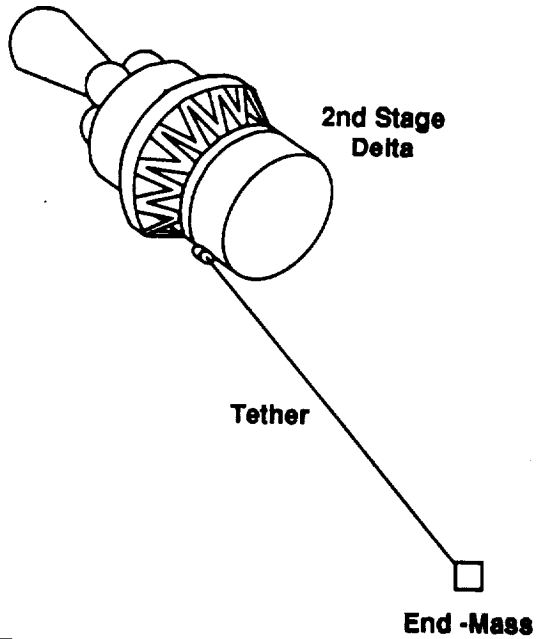

Fig. 1. SEDS End-Mass Deployed with a Tether from the Orbiting 2nd Stage of a Delta Rocket

end-mass at the end-mass. Accelerometer data when integrated can be used to infer end-mass motion (orientation) and when combined with the MSFC dynamic analyses and tether length measurements can be used to determine end-mass position (height, latitude and longitude). The field vector measured by the magnetometer data when compared to the known vector direction of the Earth's magnetic field can be used to infer end-mass orientation and roll rate; however, this requires knowledge of end-mass position. It is hoped that a combination of these measurements will allow the end-mass dynamics (position and orientation) to be determined as a function of flight time. It is the end-mass instrumentation data analysis which is addressed in this report.

ACCOMPLISHMENTS

The operation, calibration, and integration of the end-mass instrumentation were studied; calibration data for the load cell were obtained from Ray Rhew at NASA, LaRC, IRD; and calibration data for the accelerometer were obtained from Tom Finley of the same organization. At present there is no calibration data on the magnetometer. FORTRAN codes were written to convert output from these devices to engineering units. (See ANALYSIS OF SENSOR CALIBRATION DATA section of this report.) These codes were tested against calibration results obtained from Rhew and Finley and the codes were shown to perform these conversions correctly. Since there was no calibration of the magnetometer (planned for the future) the manufacture's sensitivity was used in the codes to perform these conversions. To insure that actual calibration data was available, the calibration procedures for the sensors were reviewed and a number of discussions were held with GSFC personnel concerning the future calibration of the magnetometer. A FORTRAN code was written to analyze data which is similar in format to the flight data. (See ANALYSIS OF SIMULATED FLIGHT DATA section of this report.) This flight formatting effort necessitated a complete study of the flight sensor system including the flight computer system and data storage methods. Further, a menu driven spreadsheet program was developed to list and plot the SEDS end-mass data. (See MENU DRIVEN SPREADSHEET section of this report.) This program will be helpful in distributing flight data in engineering units to the dynamics user community. A block diagram of this data analysis activity is given in Fig. 2. The last two items in

the **Dynamic Analysis** block shown in the lower right of Fig. 2 are not considered part of the scope of this work.

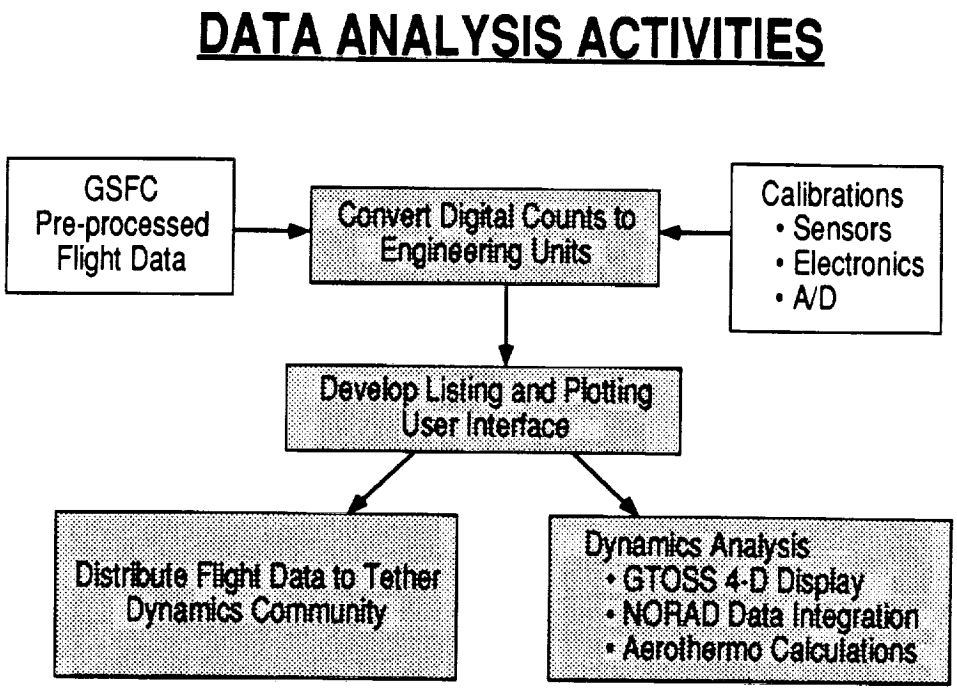

Fig. 2. Block Diagram of Data Analysis Activity

The GTOSS 4-D Display program which is used to simulate tether dynamics and end-mass orientation as a function of time was implemented on a Macintosh® computer but no simulations were performed due to lack of time and resources.

SEDS END-MASS FLIGHT SENSOR SYSTEM

System Design - A brief review of the flight sensor system is given to aid in understanding the work involved in converting sensor output to engineering units. This review is followed by a discussion of calibration, error analysis, and dynamic data analysis considerations. Shown in Fig. 3 is a block diagram of the flight sensor system. The authors would like to thank John Quinn, John Diamond and Neil Coffey for their assistance in explaining the flight electronics and flight

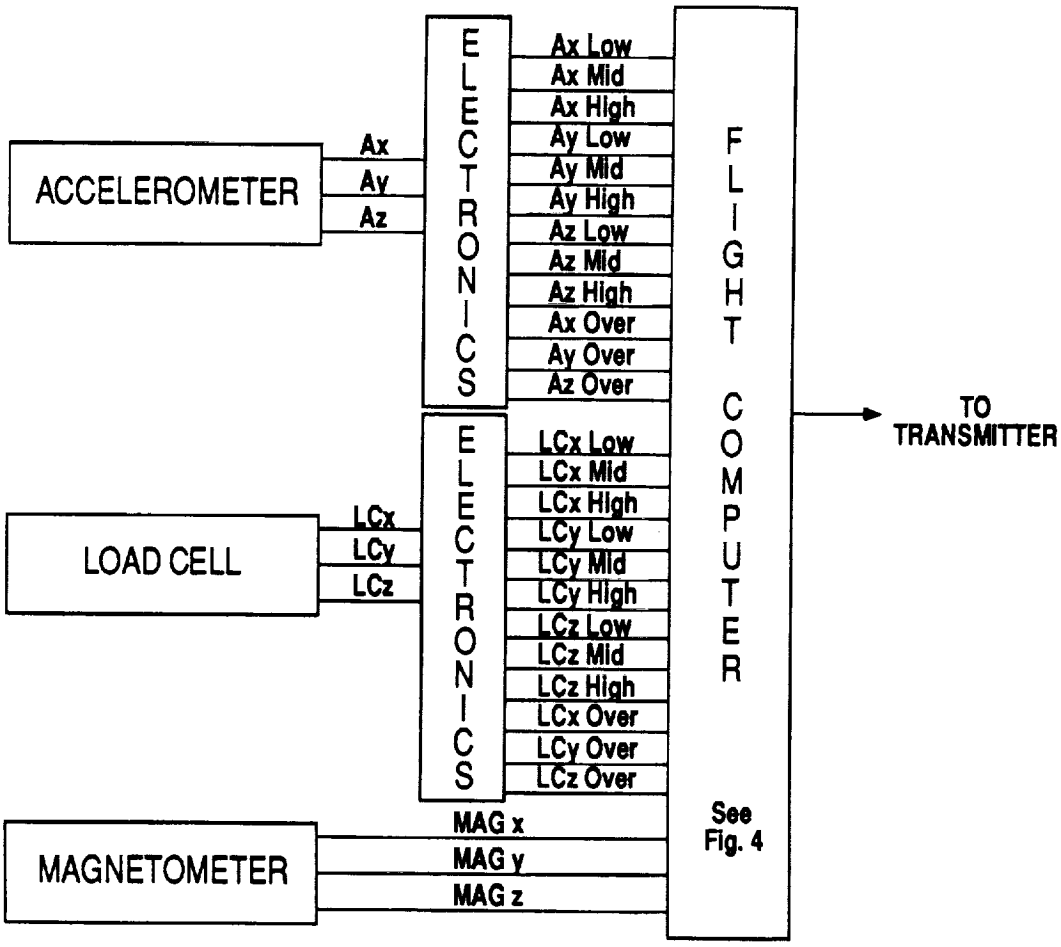

Fig. 3. Block Diagram of Flight Sensor System

computer system. The flight sensor system (See Fig. 3.) contains the three sensors, their electronics and a computer system. The load cell and accelerometer outputs require electronic processing (designed in FED) to interface with the data acquisition computer. The magnetometer is a commercially available flight unit containing its own electronics which interfaces directly with the computer. The load cell presents three signals to the load cell electronics which produces twelve signals with appropriate instrument ranges (high = +/- 10 N, medium = +/- 1 N, & low = +/- 0.1 N, & over-range = +/- 20 N). In a similar manner the accelerometer presents three signals through a filter (not shown in Fig. 3.) to its electronics which produce twelve signals with appropriate instrument ranges (high = +/- 50 mg, medium = +/- 5 mg, low = +/- 1 mg, over-range = +/- 2.5 g). The magnetometer presents three output signals to the computer with an instrument range of +/- 600 milligauss. A block diagram of the computer system was obtained from Neil Coffey of FED and is shown in Fig. 4. The first computer subsystem which the sensor/electronics, sensor diagnostics, and housekeeping outputs encounters is a multiplexer which sequentially switches their output to an A/D converter. The output from the A/D converter is presented to the CPU for logic manipulation, storage, and formatting for transmission to the ground. The computer selects the proper range for the accelerometer and load cell outputs; it puts all the sensor, sensor diagnostic, and housekeeping data in frame format; and it presents this data to the transmitter through a FIFO. The frame format for this mission is shown in Fig. 5. Each frame is one second long and contains 79 words that are 8-bits long. In these words are stored the frame number; the flight

time in hours, minutes, and seconds; 8 measurement sequences (counts and gain factor) for the accelerometer and load cell; measurement sequence for the magnetometer; and three words at the end which contain accelerometer and load

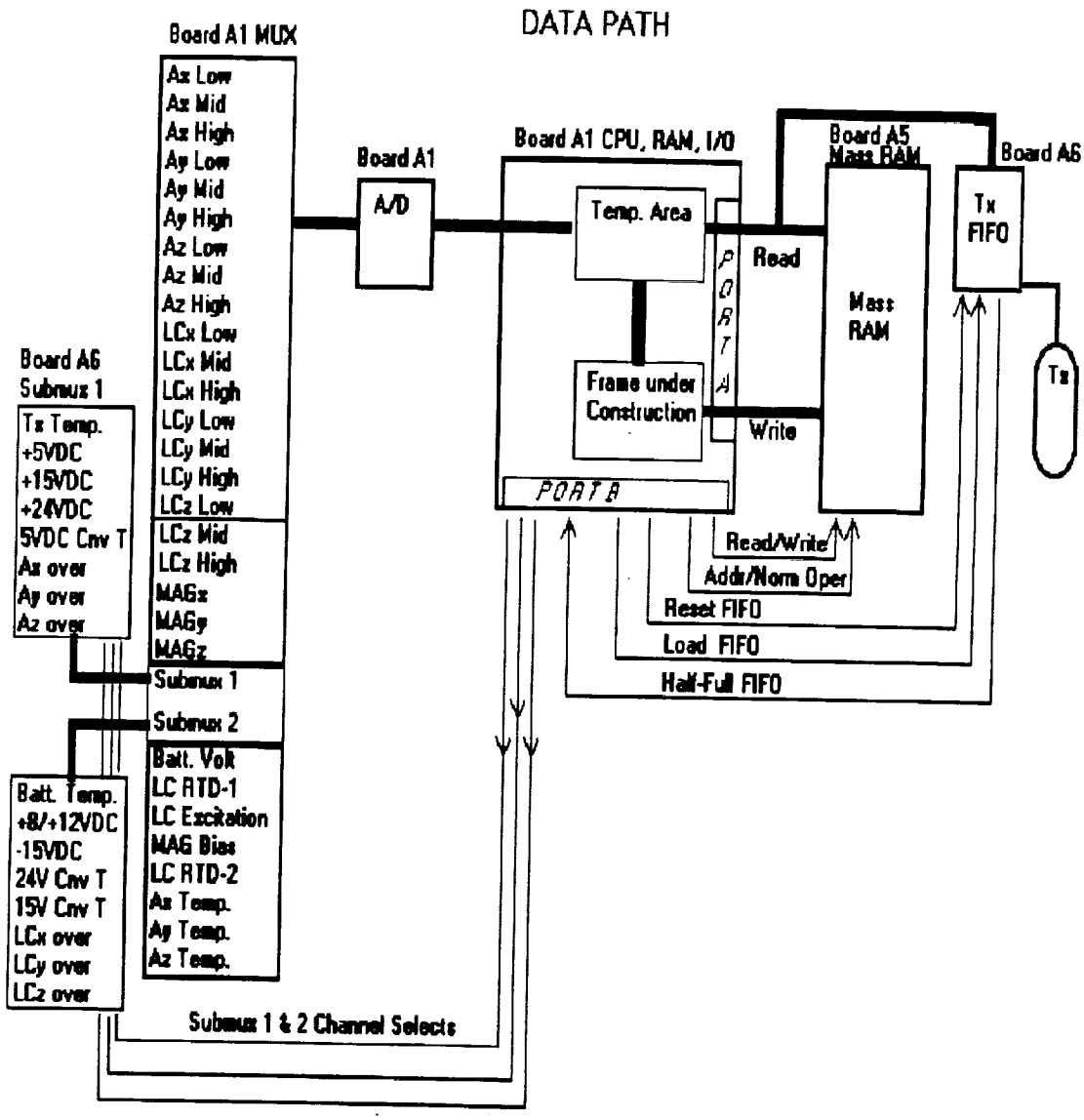

Fig. 4. Data Path Block Diagram of SEDS End-Mass Flight Computer (courtesy of Neil Coffey, FED)

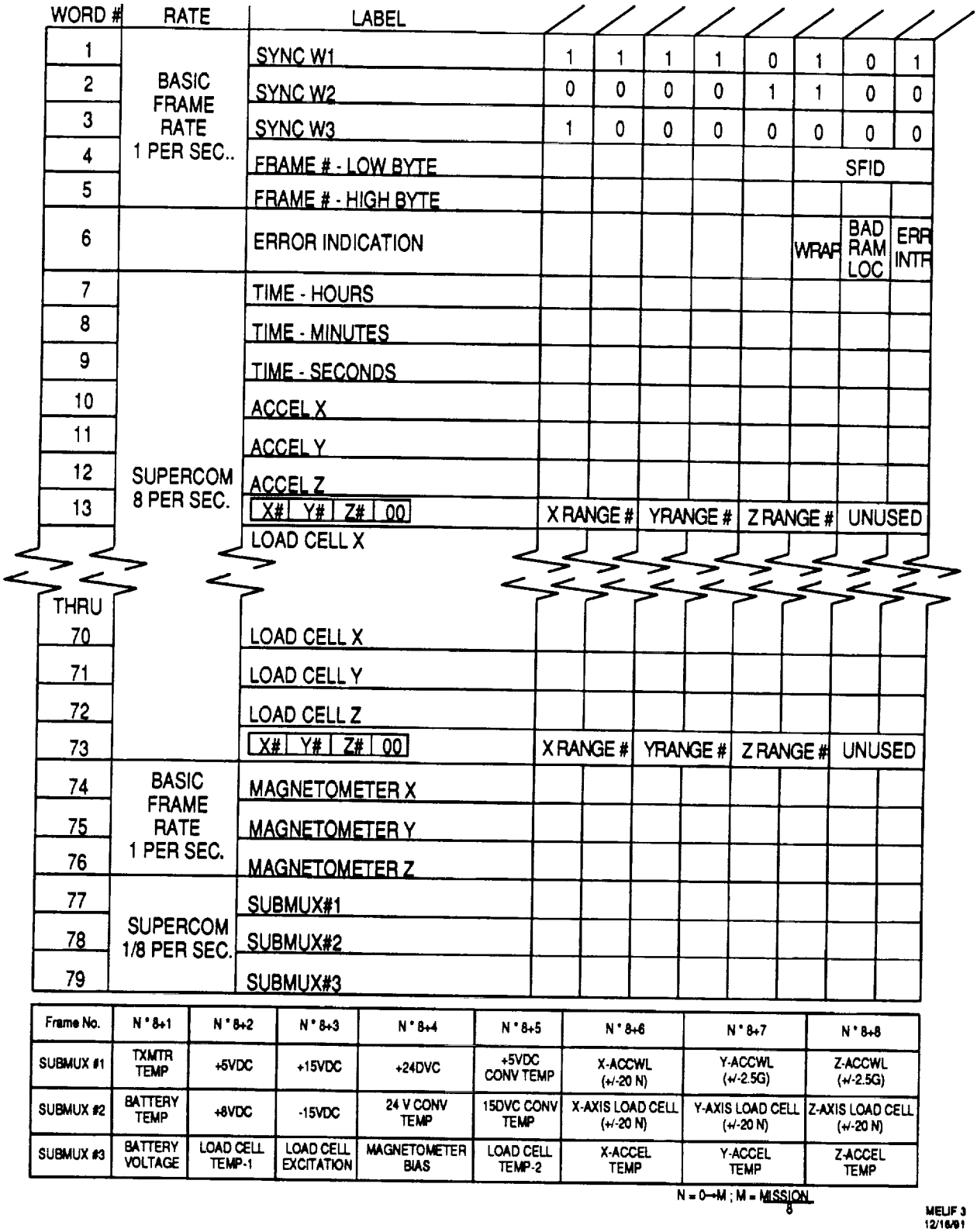

Frame No.	N * 8+1	N * 8+2	N * 8+3	N * 8+4	N * 8+5	N * 8+6	N * 8+7	N * 8+8
SUBMUX #1	TXMTR TEMP	+5VDC	+15VDC	+24DVC	+5VDC CONV TEMP	X-ACCWL (+/-20 N)	Y-ACCWL (+/-2.5G)	Z-ACCWL (+/-2.5G)
SUBMUX #2	BATTERY TEMP	+8VDC	-15VDC	24 V CONV TEMP	15DVC CONV TEMP	X-AXIS LOAD CELL (+/-20 N)	Y-AXIS LOAD CELL (+/-20 N)	Z-AXIS LOAD CELL (+/-20 N)
SUBMUX #3	BATTERY VOLTAGE	LOAD CELL TEMP-1	LOAD CELL EXCITATION	MAGNETOMETER BIAS	LOAD CELL TEMP-2	X-ACCEL TEMP	Y-ACCEL TEMP	Z-ACCEL TEMP

N = 0→M ; M = MISSION / 8

MELIF 3
12/16/91

Fig. 5. SEDS Data Frame Format (Courtesy of John Quinn, FED)

cell over-range, sensor diagnostics, and housekeeping. It requires 8 frames (or 8 seconds) to store all of the parameters contained in these last three words.

Calibration Considerations - During the contractual period, the only calibrations that were available were those for the load cell and accelerometer sensors, both without their flight electronics. (See ANALYSIS OF SENSOR CALIBRATION DATA section of this report.) Calibrations need to be made for these sensors with their electronics and these are planned for the future. The A/D transfer function needs to be determined. Since a number of the diagnostics measurements such as sensor temperature, bridge voltage, etc. are used directly in the conversion of data to engineering units, calibrations for these diagnostic devices are also required. It would also be useful to have as a verification test, a partial calibration of the entire flight system; and this test is also being planned for the future. As the data becomes available from these calibrations, the conversion programs like those in the ANALYSIS OF SENSOR CALIBRATION DATA section of this report must be modified to allow conversion to engineering units for the complete flight system data.

Error Analysis Considerations - It was planned to perform a complete error analysis for each flight sensor system; however, at present, the measurement uncertainty data is not available. This data includes uncertainties in the sensors, their electronics, the A/D converter, and the diagnostic devices. The methods of obtaining this data should be included in all calibration procedures.

Dynamic Data Analysis Considerations - In order to correlate flight data with the external environment, the times at which the actual data is obtained are required. This information is not contained in the flight data and must be reconstructed from the method used in recording the data. When this reconstruction becomes available it needs to be included in the code to calculate the correct flight time for each data point. Every 0.125 second, the data on Board A1 MUX from $A_{x\,low}$ through MAG_z (See Fig. 4.) plus one device output from each of the submux channels are recorded. Only one value of MAG_x, MAG_y, and MAG_z and one value of each of the 3 submux channels (See Fig. 5.) are recorded and stored in each one second frame. This procedure insures that the accelerometer and load cell data are equally spaced at 125 milliseconds over the one second frame time. The maximum time between the high time resolution load cell and accelerometer axes channels depends on which sensitivity range was selected and the multiplexer scan rate and is approximately 0.25 milliseconds; the maximum time between accelerometer and load cell sequences is 125 milliseconds; the maximum time from frame to frame is 1 second; and the maximum time for the accelerometer and load cell over-range and sensor diagnostics and housekeeping is 8 seconds. Data point timing has a direct effect on the dynamics analysis of the end-mass. In order to perform end-mass dynamics studies 3-axis data from the load cell, accelerometer, and magnetometer are required at the exact same time. The flight data is scanned in time and the possibility exists that data from these sensors systems can change substantially during a frame or over a 0.125 second subframe. An interpolation scheme will be needed and should be included in the codes that are sent to the dynamics user community.

SEDS END-MASS GEOMETRY

SEDS End-Mass Design - The flight hardware including the sensors, their electronics, computer, and transmitter are mounted on the SEDS baseplate. Figure 6 shows only the sensor locations on the baseplate. This figure was obtained from John Stadler of SED and the authors thank him for helping us to understand the SEDS end-mass geometry. The baseplate is approximately 12" wide by 16" long. There is a cover which is 8" high (not shown in Fig. 6). The plate is connected to the 2nd stage of the Delta rocket from below through a deployment mechanism and an isolation mechanism to limit vibration (not shown on Fig. 6). The X, Y, and Z end-mass coordinate axes are shown on the figure. The origin is at the geometric center of the plate, 1" above the plate, along the plate normal (near the center of gravity). The 3-axis accelerometer is located as near the center of gravity as possible. The X, Y, Z-axes of this device correspond to the X, Y, Z-axes of the baseplate. The load cell is shown in the upper right portion of Fig. 6 with the tether attached. Its normal axis is along the plate Z-axis; its axial axis is along the plate Y-axis; and its side axis is along the plate X-axis. The magnetometer is shown in the lower left hand portion of Fig. 6. Its X, Y, and Z-axes corresponds to the X, Y, Z-axes of the baseplate.

Dynamic Data Analysis Considerations - To derive end-mass dynamics from the end-mass sensor data a number of geometric properties of the sensors and end-mass must be known. These include: 1.) the position of each sensor with respect

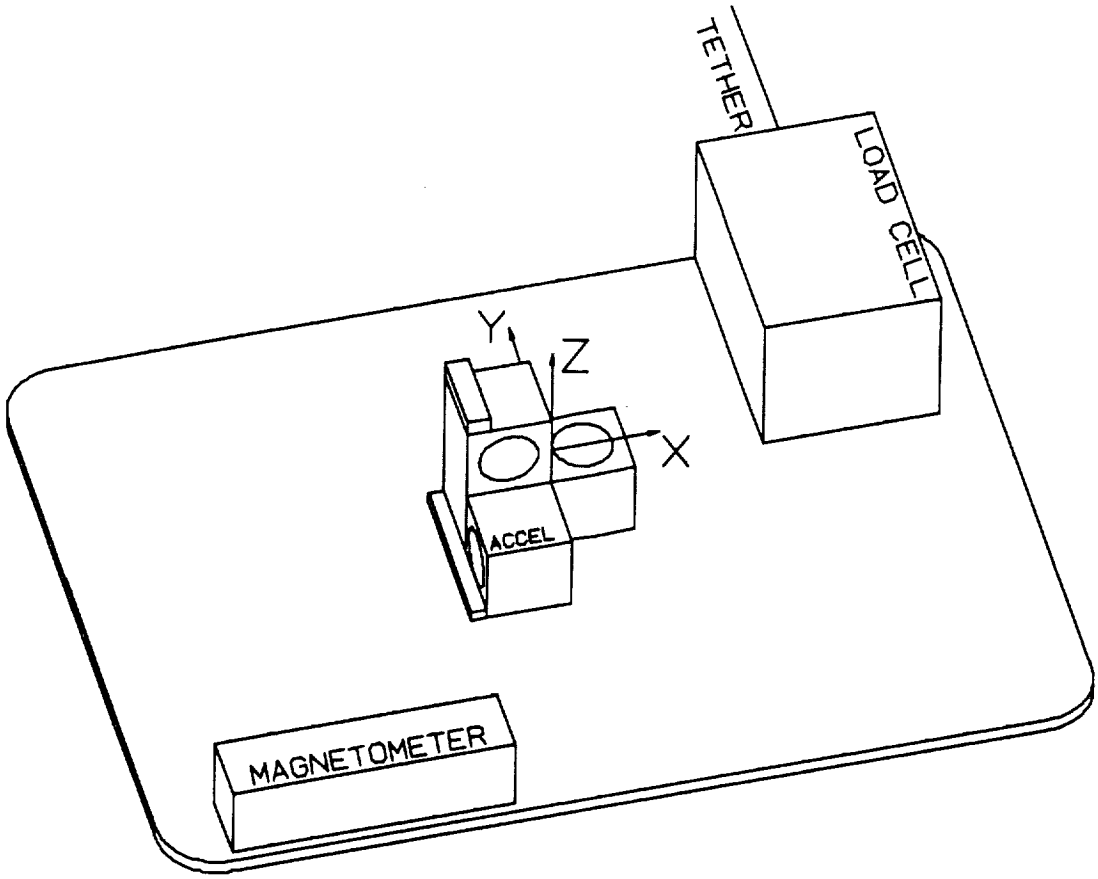

Fig. 6. SEDS End-Mass Baseplate and Sensor Geometry
(Courtesy of John Stadler, SED)

to each other and the end-mass; 2.) the sensor axes alignment in terms of the end-mass coordinate system; 3.) the overall geometry of the end-mass including the cover, deployment and isolation system; 4.) the end-mass weight; 5.) the end-mass center of gravity; and 6.) the end-mass moments of inertia (mass and products). It is planned to measure the position of the load cell and magnetometer with respect to a surface point (probably a corner) on the accelerometer. During calibrations, the axes alignment of each sensor will be measured with respect to

a convenient surface on the sensor. The accelerometer will be mounted at the geometric center of the baseplate and aligned as shown in Fig. 6. A convenient surface on the accelerometer will be chosen as the reference axis for the body (end-mass). The load cell and magnetometer will be mounted on the baseplate (as shown on Fig. 6) and their reference surfaces will be aligned with respect to the body reference axis. Their position in body coordinates and axis alignment will be measured. To get the sensor axis alignment in baseplate coordinates a coordinate transformation will be required for the accelerometer, the load cell, and the magnetometer. Either the coordinate transformation data must be made available to the dynamics user community or they must be supplied sensor data (in engineering units) in body coordinates. It appears that this second approach is the most appropriate. This would require developing a sensor transformation matrix for each code that converts flight data to engineering units. To get the overall end-mass geometry the cover and other attached devices must be measured in the baseplate coordinate system. The end-mass weight, its center of gravity, and its mass moments of inertia and products of inertia will be determined using standard engineering techniques. These geometry data have a direct impact on studies of the end-mass dynamics and should be accurately measured and supplied to the dynamic user community.

ANALYSIS OF SENSOR CALIBRATION DATA

Introduction - The instrumentation on the SEDS end-mass includes three sensors, a 3-axis load cell, a 3-axis accelerometer, and a 3-axis magnetometer. Each of these sensors has particular calibration and data analysis problems associated with the sensor physics. The load cell was fabricated in IRD under the direction of R. Rhew and is based on in-house designs used extensively in LaRC wind tunnels. It is the most complicated SEDS sensor system from a data analysis point of view since there is substantial interaction between the axes. Calibration data, interaction terms, and data analysis techniques used in this report to perform conversions to engineering units were obtained from Ray Rhew in IRD. It is also thought that the load cell is sensitive to temperature but tests have not been performed to establish this sensitivity. These tests are planned for the future and this effect must be included in data analysis. The accelerometer package consists of three independent sensors. The sensors were developed by the Sundstrand® Corporation and were purchased by Tom Finley for the SEDS mission. He is directing the effort to apply these sensors to this mission and has performed accelerometer calibrations and determined their sensitivity to temperature. These data are included in a second order fit to allow straightforward conversion to engineering units. The calibration data, temperature sensitivity, and data fit contained in this report were obtained from Tom Finley of IRD. The magnetometer was purchased by LaRC as a flight qualified item from the Develco® Corporation. At present, the magnetometer has not been calibrated;

however, calibration of this instrument will be performed at Goddard Space Flight Center (GSFC) in the future. As a place holder, the manufacturer's sensitivity is being used in a first order fit to obtain engineering units from this sensor.

Load Cell Codes - The FORTRAN code shown in Table 1. was developed, compiled with a Lahey 77® FORTRAN compiler, and run on an IBM® compatible PC. A version of this code can be found on the floppy disk attached to this report in a file named, A:\F77L\LOADCEL.FOR.

Table 1. FORTRAN code named LOADCEL.FOR Used to Convert Load Cell Data into Engineering Units.

```
      PROGRAM LOADCEL                                                    LDC001
      DIMENSION AN(25),A(25),Y(25)                                       LDC002
      OPEN(7,FILE='LOADCEL.OUT',FORM='FORMATTED',STATUS='NEW')           LDC003
C     OPEN(8,FILE='LOADCEL.INP',FORM='FORMATTED',STATUS='OLD')           LDC004
C                                                                        LDC005
C     This program takes the three output voltages from the load cell    LDC006
C     and calculates the forces in the normal, axial and side directions LDC007
C                                                                        LDC008
C     Iteration is used to obtain the solutions. The 3 forces are        LDC009
C     dimensioned.                                                       LDC010
C                                                                        LDC011
C     The program calculates the 3 forces in Lb. which are:              LDC012
C                                                                        LDC013
C     AN(I) = Force in the normal direction                              LDC014
C     A(I)  = Force in the axial direction                               LDC015
C     Y(I)  = Force in the side direction                                LDC016
C                                                                        LDC017
C     The output voltages in millivolts are                              LDC018
C                                                                        LDC019
C     TN = Output voltage in the normal direction                        LDC020
C     TA = Output voltage in the axial direction                         LDC021
C     TY = Output voltage in the side direction                          LDC022
C                                                                        LDC023
C     This section writes the header on the output file                  LDC024
C                                                                        LDC025
      WRITE(7,1)                                                         LDC026
    1 FORMAT(///,9X,'       TEST OF DATA FIT FOR TETHER LOAD CELL B',//) LDC027
      WRITE(7,2)                                                         LDC028
    2 FORMAT('           NORMAL (Z)',9X,'  AXIAL (A)',10X,' SIDE (Y)',/) LDC029
C                                                                        LDC030
C     This section reads output voltage from the input file and write    LDC031
C     them to the output file                                            LDC032
C                                                                        LDC033
C     Label 3 is the main program loop                                   LDC034
C                                                                        LDC035
    3 READ(8,4,END=9) TN,TA,TY                                           LDC036
    4 FORMAT(3F10.4)                                                     LDC037
      WRITE(7,5) TN,TA,TY                                                LDC038
    5 FORMAT(3F20.4,'       mV')                                         LDC039
C                                                                        LDC040
C     The following sensitivities & coefficients were obtained           LDC041
```

```
C     from R. Rhew in IRD (his calibration data). Sensitivity has        LDC042
C     units of mV/Lb. Unsquared coefficients are unitless.               LDC043
C     Squared coefficients have units of 1/Lb.                           LDC044
C                                                                        LDC045
C     For the normal force equations the sensitivity & coefficients are: LDC046
C                                                                        LDC047
C     CN  = Normal sensitivity                                           LDC048
C     CA  = Axial coefficient                                            LDC049
C     CY  = Side coefficient                                             LDC050
C     CN2 = Normal square coefficient                                    LDC051
C     CA2 = Axial square coefficient                                     LDC052
C     CY2 = Side square coefficient                                      LDC053
C                                                                        LDC054
      CN  = .46516                                                       LDC055
      CA  = -.31980E-02                                                  LDC056
      CY  = -.10951E-01                                                  LDC057
      CN2 = .12114E-03                                                   LDC058
      CA2 = -.52492E-03                                                  LDC059
      CY2 = .16151E-02                                                   LDC060
C                                                                        LDC061
C     For the axial force equation the sensitivity & coefficients are:   LDC062
C                                                                        LDC063
C     ACN  = Normal coefficient                                          LDC064
C     ACA  = Axial sensitivity                                           LDC065
C     ACY  = Side coefficient                                            LDC066
C     ACN2 = Normal square coefficient                                   LDC067
C     ACA2 = Axial square coefficient                                    LDC068
C     ACY2 = Side square coefficient                                     LDC069
C                                                                        LDC070
      ACN  = .21980E-01                                                  LDC071
      ACA  = .471                                                        LDC072
      ACY  = .99107E-02                                                  LDC073
      ACN2 = .32709E-03                                                  LDC074
      ACA2 = .40886E-04                                                  LDC075
      ACY2 = .53151E-03                                                  LDC076
C                                                                        LDC077
C     For the side force equation the sensitivity & coefficients are:    LDC079
C                                                                        LDC080
C     YCN  = Normal coefficient                                          LDC081
C     YCA  = Axial coefficient                                           LDC082
C     YCY  = Side sensitivity                                            LDC083
C     YCN2 = Normal square coefficient                                   LDC084
C     YCA2 = Axial square coefficient                                    LDC085
C     YCY2 = Side square coefficient                                     LDC086
C                                                                        LDC087
      YCN  = .24878E-01                                                  LDC088
      YCA  = -.84458E-02                                                 LDC089
      YCY  = .44065                                                      LDC090
      YCN2 = -.11858E-02                                                 LDC091
      YCA2 = -.22951E-03                                                 LDC092
      YCY2 = .26776E-03                                                  LDC093
C                                                                        LDC094
C     First time thru loop there are no interaction between axes         LDC095
C                                                                        LDC096
      I=1                                                                LDC097
    6 CONTINUE                                                           LDC098
      IF(I.EQ.1) THEN                                                    LDC099
      ANINTER = 0.                                                       LDC100
      AINTER  = 0.                                                       LDC101
      YINTER  = 0.                                                       LDC102
      ELSE                                                               LDC103
C                                                                        LDC104
C     Second plus all other times thru loop correction terms for         LDC105
C     interactions between axes are calculated. They are:                LDC106
C                                                                        LDC107
C     ANINTER = Normal correction caused by  axial and side forces       LDC108
C     AINTER  = Axial correction caused by normal and side forces        LDC109
C     YINTER  = Side correction caused by normal and axial forces        LDC110
C                                                                        LDC111
C     The equations for these corrections were taken from a paper        LDC112
C     obtained from R. Rhew of IRD entitled CALIBRATION AND EVALUATION   LDC113
C     OF MULTICOMPONENT STRAIN-GAGE BALANCES modified for 3-degrees      LDC114
C     of freedom                                                         LDC115
C                                                                        LDC116
C     This section calculates the nth correction terms                   LDC117
C                                                                        LDC118
      ANINTER = CN2*AN(I-1)*AN(I-1)+CA*A(I-1)                            LDC119
     1+CA2*A(I-1)*A(I-1)+CY*Y(I-1)+CY2*Y(I-1)*Y(I-1)                     LDC120
      AINTER  = ACA2*A(I-1)*A(I-1)+ACN*AN(I-1)+ACN2*AN(I-1)*AN(I-1)      LDC121
```

```
     1+ACY*Y(I-1)+ACY2*Y(I-1)*Y(I-1)                                          LDC122
      YINTER  = YCY2*Y(I-1)*Y(I-1)+YCN*AN(I-1)+YCN2*AN(I-1)*AN(I-1)           LDC123
     1+YCA*A(I-1)+YCA2*A(I-1)*A(I-1)                                          LDC124
      ENDIF                                                                   LDC125
C                                                                             LDC126
C     This section calculates corrected forces                                LDC127
C                                                                             LDC128
      AN(I) = CN*TN-ANINTER                                                   LDC129
      A(I)  = ACA*TA-AINTER                                                   LDC130
      Y(I)  = YCY*TY-YINTER                                                   LDC131
      IF(I.EQ.1) THEN                                                         LDC132
      I=I+1                                                                   LDC133
      GO TO 6                                                                 LDC134
      ENDIF                                                                   LDC135
C                                                                             LDC136
C     This section tests for convergence                                      LDC137
C                                                                             LDC138
      T1 = ABS(AN(I)-AN(I-1))                                                 LDC139
      T2 = ABS(A(I)-A(I-1))                                                   LDC140
      T3 = ABS(Y(I)-Y(I-1))                                                   LDC141
      IF(T1.LT.0.0001.AND.T2.LT.0.0001.AND.T3.LT.0.0001) GO TO 7              LDC142
      I=I+1                                                                   LDC143
      GO TO 6                                                                 LDC144
    7 CONTINUE                                                                LDC145
C                                                                             LDC146
C     This section writes to the output file the converged corrected          LDC147
C     forces                                                                  LDC148
C                                                                             LDC149
      WRITE(7,8) AN(I),A(I),Y(I)                                              LDC150
    8 FORMAT(3F20.4, '        Lb.',/)                                         LDC151
C                                                                             LDC152
C     Loops back for next set of output voltages                              LDC153
C                                                                             LDC154
      GO TO 3                                                                 LDC155
C                                                                             LDC156
C     Label 9 is END= in the READ at the beginning of the loop                LDC157
C                                                                             LDC158
    9 STOP                                                                    LDC159
      END                                                                     LDC160
```

The sensitivity and interaction terms required by LOADCEL.FOR (See line LDC046 to LDC093.) were taken from the data shown in Table 2 which were obtained from Ray Rhew. The interaction equations modified to 3-degrees of freedom (See lines LDC095 to LDC135.) were taken from NASA TN D-6860 entitled " *An Efficient Algorithm Using Matrix Methods to Solve Wind-Tunnel Force-Balance Equations* " by David L. Smith, 1972. It should be noted that the matrix technique described in this TN was not used in this code. This code uses an iterative technique. The data shown in Table 2 can be found on the floppy disk in a file named A:\F77L\LOADCEL.RRA.

Table 2. Sensitivities and Interactions for Tether Load Cell 'B' Obtained from Ray Rhew, NASA, Langley Research Center, Instrument Research Division.

```
                    Sensitivities & Interactions                                RRA001
                                                                                RRA002
COMPONENT                CALIBRATION RANGE      OUTPUT     SENSITIVITY          RRA003
NO.       NAME             LB          NT        MV/V     LB/MV/V  NT/MV/V     RRA004
                                                                                RRA005
    1     NORMAL          2.4          10.7      0.516     4.6516   20.7384     RRA006
                         -2.4         -10.7                                      RRA007
    2     AXIAL           2.4          10.7      0.510     4.7100   20.9989     RRA008
                         -2.4         -10.7                                      RRA009
    3     SIDE            2.4          10.7      0.545     4.4065   19.6456     RRA010
                         -2.4         -10.7                                      RRA011
                                                                                RRA012
                                                                                RRA013
                    NORMAL                                                      RRA014
                                    Term                EFFECT (% of F.S.)      RRA015
                    NORMAL          ---------           ---------               RRA016
                    AXIAL        -3.1980E-03             -0.32                  RRA017
                    SIDE         -1.0951E-02             -1.10                  RRA018
                                                                                RRA019
                    N^2           1.2114E-04              0.03                  RRA020
                    A^2          -5.2492E-04             -0.13                  RRA021
                    S^2           1.6151E-03              0.39                  RRA022
                                                                                RRA023
                    AXIAL                                                       RRA024
                                    Term                EFFECT (% of F.S.)      RRA025
                    NORMAL       2.1980E-02              2.20                   RRA026
                    AXIAL           ---------           ---------               RRA027
                    SIDE          9.9107E-03              0.99                  RRA028
                                                                                RRA029
                    N^2           3.2709E-04              0.08                  RRA030
                    A^2           4.0886E-05              0.01                  RRA031
                    S^2           5.3151E-04              0.13                  RRA032
                                                                                RRA033
                    SIDE                                                        RRA034
                                    Term                EFFECT (% of F.S.)      RRA035
                    NORMAL       2.4878E-02              2.49                   RRA036
                    AXIAL        -8.4458E-03             -0.84                  RRA037
                    SIDE            ---------           ---------               RRA038
                                                                                RRA039
                    N^2          -1.1858E-03             -0.28                  RRA040
                    A^2          -2.2951E-04             -0.06                  RRA041
                    S^2           2.6776E-04              0.06                  RRA042
```

The code shown in Table 1 requires an input file named LOADCEL.INP which contains the output voltages in mV for each axis of the load cell in order; normal, axial, and side. (See line LDC004 and LDC036.) This input file is displayed in Table 3, is based on data found in Table 5, and can be found on the floppy disk in a file named A:\F77L\LOADCEL.INP.

Table 3. Input File Named LOADCEL.INP Required for Code Shown in Table 1.

```
 5.1610    0.1160    0.1200                                    INP001
-5.1580   -0.1080   -0.1510                                    INP002
-0.0230    5.0960   -0.0490                                    INP003
 0.0100   -5.0950    0.0430                                    INP004
-0.0360    0.0570    5.4500                                    INP005
 0.0760   -0.0440   -5.4430                                    INP006
-0.0100   -3.5640    3.8980                                    INP007
-0.0230    3.6320    3.8190                                    INP008
-3.6720    2.5050    2.6130                                    INP009
```

The code shown in Table 1 produces an output file (See line LDC003.) named LOADCEL.OUT which contains the sensor output in mV (read from the input file) and the corrected force in Lb. for all three axes. This output file is displayed in Table 4 and can be found on the floppy disk in a file named A:\F77L\LOADCEL.OUT.

Table 4. Output File Named LOADCEL.OUT Produced by Code Shown in Table 1.

```
          TEST OF DATA FIT FOR TETHER LOAD CELL B                OUT001
                                                                 OUT002
                                                                 OUT003
NORMAL (Z)          AXIAL (A)          SIDE (Y)                  OUT004
                                                                 OUT005
   5.1610              0.1160             0.1200      mV        OUT006
   2.4000              0.0000             0.0000      Lb.       OUT007
                                                                 OUT008
  -5.1580             -0.1080            -0.1510      mV        OUT009
  -2.4000              0.0000             0.0000      Lb.       OUT010
                                                                 OUT011
  -0.0230              5.0960            -0.0490      mV        OUT012
   0.0000              2.4000             0.0000      Lb.       OUT013
                                                                 OUT014
   0.0100             -5.0950             0.0430      mV        OUT015
   0.0000             -2.4000             0.0000      Lb.       OUT016
                                                                 OUT017
  -0.0360              0.0570             5.4500      mV        OUT018
   0.0002              0.0000             2.4000      Lb.       OUT019
                                                                 OUT020
   0.0760             -0.0440            -5.4430      mV        OUT021
  -0.0002              0.0000            -2.4000      Lb.       OUT022
                                                                 OUT023
  -0.0100             -3.5640             3.8980      mV        OUT024
   0.0054             -1.6973             1.7031      Lb.       OUT025
                                                                 OUT026
  -0.0230              3.6320             3.8190      mV        OUT027
   0.0101              1.6920             1.6968      Lb.       OUT028
                                                                 OUT029
  -3.6720              2.5050             2.6130      mV        OUT030
  -1.6929              1.2033             1.2070      Lb.       OUT031
```

Shown in Table 5 are calibration results obtained from R. Rhew for all three axes of Load Cell 'B'. This data can be found on the floppy disk in a file named A:\F77L\LOADCEL.RRB.

Table 5. Calibration Results for the Tether Load Cell 'B' Obtained from Ray Rhew, NASA, Langley Research Center, Instrumentation Division.

CALIBRATION RESULTS FOR THE TETHER LOAD CELL 'B'				
NORMAL (Z)	AXIAL (Y)	SIDE (X)		
5.1610	0.1160	0.1200	Millivolts	RRB005
2.4000	0.0000	0.0000	Applied Load	RRB006
2.4007	0.0546	0.0529	Uncorrected Load	RRB007
0.0007	0.0546	0.0529	Correction	RRB008
2.4000	0.0000	0.0000	Corrected Load	RRB009
0.00	-0.00	-0.00	Difference % F.S.	RRB010
-5.1580	-0.1080	-0.1510	Millivolts	RRB013
-2.4000	0.0000	0.0000	Applied Load	RRB014
-2.3993	-0.0509	-0.0665	Uncorrected Load	RRB015
0.0007	-0.0509	-0.0665	Correction	RRB016
-2.4000	-0.0000	-0.0000	Corrected Load	RRB017
-0.00	0.00	0.00	Difference % F.S.	RRB018
-0.0230	5.0960	-0.0490	Millivolts	RRB021
0.0000	2.4000	0.0000	Applied Load	RRB022
-0.0107	2.4002	-0.0216	Uncorrected Load	RRB023
-0.0107	0.0002	-0.0216	Correction	RRB024
-0.0000	2.4000	-0.0000	Corrected Load	RRB025
0.00	0.00	0.00	Difference % F.S.	RRB026
0.0100	-5.0950	0.0430	Millivolts	RRB029
0.0000	-2.4000	0.0000	Applied Load	RRB030
0.0047	-2.3997	0.0189	Uncorrected Load	RRB031
0.0047	0.0002	0.0189	Correction	RRB032
-0.0000	-2.4000	0.0000	Corrected Load	RRB033
0.00	-0.00	-0.00	Difference % F.S.	RRB034
-0.0360	0.0570	5.4500	Millivolts	RRB037
0.0000	0.0000	2.4000	Applied Load	RRB038
-0.0167	0.0268	2.4015	Uncorrected Load	RRB039
-0.0170	0.0269	0.0015	Correction	RRB040
0.0002	-0.0000	2.4000	Corrected Load	RRB041
-0.01	0.00	0.00	Difference % F.S.	RRB042
0.0760	-0.0440	-5.4430	Millivolts	RRB045
0.0000	0.0000	-2.4000	Applied Load	RRB046
0.0354	-0.0207	-2.3985	Uncorrected Load	RRB047
0.0356	-0.0207	0.0015	Correction	RRB048
-0.0002	0.0000	-2.4000	Corrected Load	RRB049
0.01	-0.00	-0.00	Difference % F.S.	RRB050
-0.0100	-3.5640	3.8980	Millivolts	RRB053
0.0000	-1.6970	1.6970	Applied Load	RRB054
-0.0047	-1.6786	1.7177	Uncorrected Load	RRB055
-0.0101	0.0187	0.0146	Correction	RRB056
0.0054	-1.6973	1.7031	Corrected Load	RRB057
-0.24	0.01	-0.27	Difference % F.S.	RRB058

				RRB060
-0.0230	3.6320	3.8190	Millivolts	RRB061
0.0000	1.6970	1.6970	Applied Load	RRB062
-0.0107	1.7107	1.6828	Uncorrected Load	RRB063
-0.0208	0.0187	-0.0139	Correction	RRB064
0.0101	1.6920	1.6968	Corrected Load	RRB065
-0.45	0.22	0.01	Difference % F.S.	RRB066
				RRB067
				RRB068
-3.6720	2.5050	2.6130	Millivolts	RRB069
-1.6970	1.2000	1.2000	Applied Load	RRB070
-1.7081	1.1799	1.1514	Uncorrected Load	RRB071
-0.0151	-0.0235	-0.0556	Correction	RRB072
-1.6929	1.2033	1.2070	Corrected Load	RRB073
-0.18	-0.15	-0.31	Difference % F.S.	RRB074

These codes have not been thoroughly tested due to lack of time and resources; however, a comparison of lines INP001, INP002, INP003, INP004, INP005, INP006, INP007, INP008, INP009 in Table 3 with lines RRB005, RRB013, RRB021, RRB029, RRB037, RRB045, RRB053, RRB061, RRB069 in Table 5, respectively establishes that the input data are the same as that obtained from Ray Rhew. A similar comparison of lines OUT007, OUT010, OUT013, OUT016, OUT019, OUT022, OUT025, OUT028, OUT031 in Table 4 with lines RRB009, RRB017, RRB025, RRB033, RRB041, RRB049, RRB057, RRB065, RRB073 in Table 5, respectively establishes that the code in Table 1 produces the same output as that produced by Ray Rhew.

Load Cell Future Work - The following tasks should be accomplished in the future to insure reliable data analysis. These recommendations are summarized in the last section of this report.

1. A test plan should be developed to further validate these codes.
2. Electronic calibrations and temperature sensitivities should be included in the codes to allow a complete analysis of the load cell data.
3. A load cell temperature interpolation scheme needs to be developed since flight temperature measurements are not recorded as often (once every 8 seconds) as the actual load cell data (8 per second).

4. A load cell output-time interpolation scheme needs to be developed in case there are significant changes in output in the millisecond time frame during the flight. This scheme is required since simultaneous outputs from all three axes are required to convert the load cell data to engineering units.

5. To give the sensor data (in engineering units) in body coordinates, a coordinate transformation matrix must be developed and included in the codes.

6. A complete load cell system error analysis is required to establish actual measurement accuracy of the instrument in flight configuration so as not to draw erroneous conclusions when dynamic analysis is performed. This is particularly true for tether angle calculations.

7. Measurement uncertainty data is required to perform the error analysis described in item 5 above. To insure that this data is available, coordination with a number of developers at LaRC, including the sensor developer in IRD and the electronic and data handling developers and engineers in FED, will be required. A review of calibration and test procedures should be conducted to insure that the necessary error analysis data are being measured.

8. The format for the flight data will have to be determined and the codes modified to include this format in reading the input data. GSFC has the task of reading the actual flight data and converting it to a format suitable for analysis.

9. The output format from the codes will have to be modified to meet the requirements of the dynamics analysis user community. A possible example of a format is given in the Table 15 of this report.

Accelerometer Codes - The FORTRAN code shown in Table 6. was developed, compiled with a Lahey 77® FORTRAN compiler, and run on an IBM® compatible PC. A version of this code can be found on the floppy disk attached to this report in a file named, A:\F77L\ACCLERA.FOR.

Table 6. FORTRAN Code Named ACCLERA.FOR Used to Convert Accelerometer Data into Engineering Units.

```
      PROGRAM ACCLERA                                                    ACC001
      OPEN(7,FILE='ACCLERA.OUT',FORM='FORMATTED',STATUS='NEW')           ACC002
      OPEN(8,FILE='ACCLERA.INP',FORM='FORMATTED',STATUS='OLD')           ACC003
C                                                                        ACC004
C     This program takes the output voltages from the accelerometer      ACC005
C     and calculates acceleration                                        ACC006
C                                                                        ACC007
C     Output from the program is acceleration in g's (ACC)               ACC008
C                                                                        ACC009
C     The output voltage in volts is (AOUTPUT)                           ACC010
C                                                                        ACC011
C     This section writes header on output file                          ACC012
C                                                                        ACC013
      WRITE(7,6)                                                         ACC014
    6 FORMAT(///,9X,'TEST OF DATA FIT FOR SUNDSTRAND ACCELEROMETER',     ACC015
     1' SER.NO. 534',//)                                                 ACC016
      WRITE(7,7)                                                         ACC017
    7 FORMAT(7X,'TEMP. SENSOR (microA)',4X,'OUTPUT (V)',10X,             ACC018
     1'ACCLERATION (g)',/)                                               ACC019
C                                                                        ACC020
C     This section reads temperature sensor current and accelerometer    ACC021
C     output voltage from the input file                                 ACC022
C                                                                        ACC023
C     Label 9 is the main program loop                                   ACC024
C                                                                        ACC025
    9 READ(8,4,END=20) TS,AOUTPUT                                        ACC026
    4 FORMAT(F10.3,F10.6)                                                ACC027
C                                                                        ACC028
C     The following coefficients were obtained from Tom Finley of IRD    ACC029
C     (from his accelerometer calibration).                              ACC030
C                                                                        ACC031
C     BCONT2 = Bias squared temp. coefficient                            ACC032
C     BCONT1 = Bias temp. coefficient                                    ACC033
C     BCON   = Bias coefficient                                          ACC034
C                                                                        ACC035
      BCONT2 = 5.59614E-08                                               ACC036
      BCONT1 = -3.457095E-05                                             ACC037
      BCON   = 6.999659E-03                                              ACC038
C                                                                        ACC039
C     SENCONT = Sensitivity temp. coefficient                            ACC040
C     SENCON  = Sensitivity coefficient                                  ACC041
C                                                                        ACC042
```

```
      SENCONT = 1.141304E-04                                              ACC043
      SENCON  = 1.241903                                                  ACC044
C                                                                         ACC045
C     TS      = Temperature sensor output (microA)                        ACC046
C                                                                         ACC047
C     This section calculates acceleration                                ACC048
C                                                                         ACC049
C     The equations for calculating accelerations were taken from         ACC050
C     T. Finley's data sheet entitled NASA-LRC-INSTRUMENTATION,           ACC051
C     REPORT ON ACCELEROMETER                                             ACC052
C                                                                         ACC053
      BIAS = BCONT2*TS*TS+BCONT1*TS+BCON                                  ACC054
      SENS = SENCONT*TS+SENCON                                            ACC055
      ACC = (AOUTPUT-BIAS)/SENS                                           ACC056
C                                                                         ACC057
C     This section writes to output file                                  ACC058
C                                                                         ACC059
      WRITE(7,5) TS,AOUTPUT,ACC                                           ACC060
    5 FORMAT(F20.3,F20.6,F20.6)                                           ACC061
C                                                                         ACC062
C     Loops back for next set of data points                              ACC063
C                                                                         ACC064
      GO TO 9                                                             ACC065
C                                                                         ACC066
C     Label 20 is END= in the READ at the beginning of the loop           ACC067
C                                                                         ACC068
   20 STOP                                                                ACC069
      END                                                                 ACC070
```

The second-order fit with coefficients required by this code (See line ACC029 to ACC057.) was taken from the data shown in Table 7 which was obtained from Tom Finley. The data shown in Table 7 can be found on the floppy disk in a file named A:\F77L\ACCLERA.TFA.

Table 7. Page 1 of a Report on Accelerometer Serial Number 534 Obtained from Tom Finley, NASA, Langley Research Center, Instrument Research Division.

```
                NASA-LRC-INSTRUMENT RESEARCH DIVISION      Sheet 1 of25   TFA001
                                                                          TFA002
                      REPORT ON ACCELEROMETER                             TFA003
                                                                          TFA004
                                                                          TFA005
Mfg. SUNDSTRAND          Model QA2000          SER.No. 534                TFA006
                                                                          TFA007
DATE 8/16/90             Cal. By 2675          Approved RF                TFA008
                                                                          TFA009
                                                                          TFA010
TS = TEMPERATURE SENSOR OUTPUT (microA)                                   TFA011
OUTPUT = ACCELEROMETER OUTPUT (VOLTS)                                     TFA012
                                                                          TFA013
SENSITIVITY (V/G) = 1.141304E-04 * (TS) + 1.241903                        TFA014
BIAS (VOLTS) = 5.59614E-08 * (TS) ^ 2 - 3.457095E-05 * (TS)               TFA015
+ 6.999659E-03                                                           TFA106
ACCELERATION (G) = (OUTPUT - BIAS) / SENSITIVITY                          TFA017
```

The code shown in Table 6 requires an input file named ACCLERA.INP (See line ACC003 and ACC026.) which contains the output from the temperature sensors in microA (1st column) and the accelerometer output in voltage (2nd column). This input file is displayed in Table 8, is based on data found in Table 10, and can be found on the floppy disk in a file named A:\F77L\ACCLERA.INP.

Table 8. Input File Named ACCLERA.INP Required for FORTRAN Code Shown in Table 6.

```
259.289  0.017140                                    INA001
279.712  0.017073                                    INA002
304.584  0.017066                                    INA003
314.654  0.017063                                    INA004
259.289  1.273308                                    INA005
279.712  1.275394                                    INA006
304.584  1.278235                                    INA007
314.654  1.279533                                    INA008
259.289 -0.013543                                    INA009
279.712 -0.013657                                    INA010
304.584 -0.013743                                    INA011
314.654 -0.013738                                    INA012
259.289 -1.269649                                    INA013
279.712 -1.271869                                    INA014
304.584 -1.274797                                    INA015
314.654 -1.276074                                    INA016
```

The code shown in Table 6 produces an output file (See line ACC002.) named ACCLERA.OUT which contains the temperature sensor output in microA, the accelerometer output in Volts (both read from the input file), and the calculated acceleration in g's. This output file is displayed in Table 9 and can be found on the floppy disk named A:\F77L\ACCLERA.OUT. Shown in Table 10 are calibration results obtained from Tom Finley for the same accelerometer. This data can be found on the floppy disk named A:\F77L\ACCLERA.TFB.

Table 9. Output File Named ACCLERA.OUT Produced by FORTRAN Code Shown in Table 6.

```
TEST OF DATA FIT FOR SUNDSTRAND ACCELEROMETER SER.NO. 534          OUA001
                                                                   OUA002
                                                                   OUA003
TEMP. SENSOR (microA)     OUTPUT (V)          ACCELERATION (g)     OUA004
                                                                   OUA005
      259.289             0.017140            0.012066           OUA006
      279.712             0.017073            0.012062           OUA007
      304.584             0.017066            0.012066           OUA008
      314.654             0.017063            0.012052           OUA009
      259.289             1.273308            1.000011           OUA010
      279.712             1.275394            0.999889           OUA011
      304.584             1.278235            0.999928           OUA012
      314.654             1.279533            1.000044           OUA013
      259.289            -0.013543           -0.012065           OUA014
      279.712            -0.013657           -0.012062           OUA015
      304.584            -0.013743           -0.012066           OUA016
      314.654            -0.013738           -0.012052           OUA017
      259.289            -1.269649           -0.999962           OUA018
      279.712            -1.271869           -0.999804           OUA019
      304.584            -1.274797           -0.999838           OUA020
      314.654            -1.276074           -0.999939           OUA021
```

Table 10. Page 4 of a Report on Accelerometer Serial Number 534 Obtained from Tom Finley, NASA, Langley Research Center, Instrumentation Division.

```
                NASA-LRC-INSTRUMENT RESEARCH DIVISION        Sheet 4 of25   TFB001
                                                                            TFB002
                        REPORT ON ACCELEROMETER                             TFB003
                                                                            TFB004
                                                                            TFB005
Mfg. SUNDSTRAND          Model QA2000          SER.No. 534                  TFB006
                                                                            TFB007
DATE 8/16/90             Cal. By 2675          Approved RF                  TFB008
                                                                            TFB009
INPUT (G) = SIN(ANGLE + OFFSET)                                             TFB010
CALCULATED (G) = (OUTPUT - BIAS) / SENSITIVITY                              TFB011
                                                                            TFB012
TEMP. SENSOR    ANGLE      OUTPUT       INPUT      CALCULATED     ERROR    TFB013
  (microA)    (DEGREES)  (VOLTS dc)      (G)          (G)        (microG)  TFB014
                                                                            TFB015
  259.289         0       0.017140    0.012066    0.012066         -0      TFB016
  279.712         0       0.017073    0.012064    0.012062         -2      TFB017
  304.584         0       0.017066    0.012068    0.012066         -1      TFB018
  314.654         0       0.017063    0.012052    0.012052         -0      TFB019
  259.289        90       1.273308    0.999927    1.000011         84      TFB020
  279.712        90       1.275394    0.999927    0.999890        -37      TFB021
  304.584        90       1.278235    0.999927    0.999928          1      TFB022
  314.654        90       1.279533    0.999927    1.000044        117      TFB023
  259.289       180      -0.013543   -0.012066   -0.012066          0      TFB024
  279.712       180      -0.013657   -0.012064   -0.012062          2      TFB025
  304.584       180      -0.013743   -0.012068   -0.012066          1      TFB026
  314.654       180      -0.013738   -0.012052   -0.012052          0      TFB027
  259.289       270      -1.269649   -0.999927   -0.999962        -35      TFB028
  279.712       270      -1.271869   -0.999927   -0.999804        123      TFB029
  304.584       270      -1.274797   -0.999927   -0.999838         89      TFB030
  314.654       270      -1.276074   -0.999927   -0.999939        -12      TFB031
```

These codes have not been thoroughly tested due to lack of time and resources: however, a comparison of the data in the 1st column of Table 8 with the 1st column in Table 10 and the 2nd column in Table 8 with the 3rd column in Table 10 establishes that the input data is the same as that obtained from Tom Finley. A similar comparison between the data in the 3rd column in Table 9 and the 5th column in Table 10 establishes that the code in Table 6 produces the same output as that produced by Tom Finley.

Accelerometer Future Work - The following tasks should be accomplished in the future to insure reliable data analysis. These recommendations are summarized in the final section of this report.

1. A test plan should be developed to further validate these codes.
2. Electronic calibrations should be included in the codes to allow a complete analysis of the accelerometer data.
3. To give the sensor data (in engineering units) in body coordinates, a coordinate transformation matrix must be developed and included in the codes.
4. A complete accelerometer system error analysis is required to establish measurement accuracy so as not to draw erroneous conclusions when dynamic analysis is performed.
5. Measurement uncertainty data are required to perform the error analysis described in item 3 above. To insure that this data is available, coordination with a number of developers at LaRC including the sensor

developer in IRD and the electronic and data handling developer and engineers in FED will be required. A review of calibration and test procedures should be conducted to insure that the necessary error analysis data are being measured.

6. The format for the flight data will have to be determined and the codes modified to include this format in reading the input data. GSFC has the task of reading the actual flight data and converting it to a format suitable for analysis.

7. The output format from the codes will have to be modified to meet the requirements of the dynamics analysis user community. A possible example of a format is given in Table 15 of this report.

Magnetometer Codes - The FORTRAN code shown in Table 11 was developed, compiled with a Lahey 77® FORTRAN compiler, and run on an IBM® compatible PC. This code is only a place holder (See **Magnetometer Future Work** subsection.) since the magnetometer has not been calibrated. There are plans to calibrate this instrument at GSFC in the future. It is expected that the magnetometer is linear and that this calibration will produce an accurate sensitivity for this sensor.

Table 11. FORTRAN Code (Place Holder) Named MAGNO.FOR Used to Convert Magnetometer Data into Engineering Units.

```
      PROGRAM MAGNO                                                     MAG001
C                                                                       MAG002
C     File name = MAGNO.FOR                                             MAG003
C                                                                       MAG004
C     This program is basically a place holder program since no         MAG005
C     calibrations have been done on the magnetometer. When this        MAG006
C     data is available (probably a second order fit), it can be        MAG007
C     substituted in the calculation section of the code.               MAG008
C                                                                       MAG009
      OPEN(7,FILE='MAGNO.OUT',FORM='FORMATTED',STATUS='NEW')            MAG010
      OPEN(8,FILE='MAGNO.INP',FORM='FORMATTED',STATUS='OLD')            MAG011
C                                                                       MAG012
C     This program takes the output voltage from the magnetometer       MAG013
C     and calculates magnetic field strength using the manufacturer's   MAG014
C     (DEVELCO 9200 Series) sensitivity.                                MAG015
C                                                                       MAG016
C     Output from the program is magnetic field strength in             MAG017
C     mgauss (AMFS)                                                     MAG018
C                                                                       MAG019
C     The output voltage in volts is (AOUTMAG)                          MAG020
C                                                                       MAG021
C     This section writes header on output file                         MAG022
C                                                                       MAG023
      WRITE(7,6)                                                        MAG024
    6 FORMAT(///,15X,'DEVELCO MAGNETOMETER S-9200 Not Calibrated',//)   MAG025
      WRITE(7,7)                                                        MAG026
    7 FORMAT(7X,'OUTPUT VOLTAGE (V)            MAGNETIC FS (mgause)',/) MAG027
C                                                                       MAG028
C     This section reads output voltage from the input file.            MAG029
C                                                                       MAG030
C     Label 9 is the main program loop                                  MAG031
C                                                                       MAG032
    9 READ(8,4,END=20) AOUTMAG                                          MAG033
    4 FORMAT(F10.3)                                                     MAG034
C                                                                       MAG035
C     The following coefficients were obtained using a linear fit       MAG036
C     and the manufacture's sensitivity. 0V = -600mgause, 5V = 600mgause MAG037
C                                                                       MAG038
      CONA =  240.                                                      MAG039
      CON  = -600.                                                      MAG040
C                                                                       MAG041
C     This section calculates magnetic field strength                   MAG042
C                                                                       MAG043
      AMFS = CONA*AOUTMAG + CON                                         MAG044
C                                                                       MAG045
C     This section writes output voltage and magnetic field strength    MAG046
C     to the output file                                                MAG047
C                                                                       MAG048
      WRITE(7,5) AOUTMAG,AMFS                                           MAG049
    5 FORMAT(F20.3,10X,F20.3)                                           MAG050
C                                                                       MAG051
C     Loops back for next set of data                                   MAG052
C                                                                       MAG053
      GO TO 9                                                           MAG054
C                                                                       MAG055
C     Label 20 is END= in the READ at the beginning of the loop         MAG056
C                                                                       MAG057
   20 STOP                                                              MAG058
      END                                                               MAG059
```

A version of this code can be found on the floppy disk attached to this report under the name, A:\F77L\MAGNO.FOR. The sensitivity required by this code for the first-order fit of magnetic field strength to output voltage (See line MAG036 to MAG045.) was taken from the manufacturer's operation manual. The code (Table 11) requires an input file named MAGNO.INP (See line MAG011 and MAG033.) which contains the magnetometer output voltage in volts. This input file is displayed in Table 12; it is based on plus and minus full scale, plus and minus half scale, and zero; and it can be found on the floppy disk in a file named A:\F77L\MAGNO.INP.

Table 12. Input File Named MAGNO.INP Required for Code Shown in Table 11.

```
0.000                                                    INB.001
1.250                                                    INB.002
2.500                                                    INB.003
3.750                                                    INB.004
5.000                                                    INB.005
```

The code shown in Table 11 produces an output file (See line MAG010.) named MAGNO.OUT which contains the magnetometer output in Volts (read from the input file) and the calculated magnetic field strength in milligauss. This output file is displayed in Table 13 and can be found on the floppy disk named A:\F77L\MAGNO.OUT. It can be seen from the data in Table 13 that the code in Table 11 calculates plus and minus full and half scale, and zero magnetic field strength for the given range of output voltage.

Table 13. Output File Named MAGNO.OUT Produced by Code Shown in Table 11.

```
        DEVELCO MAGNETOMETER S-9200 Not Calibrated                    OUB001
                                                                      OUB002
                                                                      OUB003
OUTPUT VOLTAGE (V)          MAGNETIC FS (milligause)                  OUB004
                                                                      OUB005
          0.000                    -600.000                           OUB006
          1.250                    -300.000                           OUB007
          2.500                       0.000                           OUB008
          3.750                     300.000                           OUB009
          5.000                     600.000                           OUB010
```

Magnetometer Future Work - The following tasks should be accomplished in the future to insure reliable data analysis. These recommendations are summarized in the final section of this report.

1. Test and calibration data for the magnetometer are needed. Calibration procedures must be developed and documented before the instrument is calibrated at GSFC. Temperature sensitivity should be determined to allow a complete analysis of the magnetometer data.
2. After the magnetometer is calibrated, a code should be written to allow magnetometer data analysis. This code will probably be similar to the accelerometer code found in Table 6.
3. A test plan should be developed to test the code proposed in item 2.
4. To give the sensor data (in engineering units) in body coordinates, a coordinate transformation matrix must be developed and included in the codes.
5. Codes need to be written to derive SEDS end mass orientation from a comparison of the Earth's magnetic field and the magnetic field derived from the magnetometer data. This comparision will require the use of an Earth's magnetic field model.

6. A complete magnetometer system error analysis is required to establish measurement accuracy so as not to draw erroneous conclusions when dynamic analysis is performed. This is particularly true for orientation calculations.

7. Measurement uncertainty data is required to perform the error analysis described in item 5 above. To insure that these data are available, coordination with GSFC test and calibration personal will be required. The calibration and test procedures should require that the necessary error analysis data be measured.

8. The format for the flight data will have to be determined and the codes developed to include this format in reading the flight input data. GSFC has the task of reading the actual flight data and converting it to a format suitable for analysis.

9. The output format from the codes will have to be developed to meet the requirements of the dynamics analysis user community.

ANALYSIS OF SIMULATED FLIGHT DATA

Introduction - The code shown in this section of this report was developed to analyze sensor data that is similar to the actual flight data. The flight data required to perform this analysis consists of the following: time in hours, minutes, and seconds; X-axis counts and gain factor; Y-axis counts and gain factor; Z-axis counts and gain factor; and sensor temperature. The magnetometer does not have a gain factor. There are two temperature sensors for the load cell and one temperature sensor for each accelerometer (three total). The flight data format is divided into 1 second frames. During each frame the outputs and gains for each axis of the load cell and accelerometer are recorded 8 times. The outputs for each axis of the magnetometer are recorded once. The temperatures for these sensors are recorded once each 8 frames. Using this information, a format was developed for each of the sensors and given to Tom Finley and his student, Laura Stobie. They developed a set of data files containing simulated flight data. This data was then used as input to the code shown in Table 14. Originally it was expected that data would be available for all of the sensors; however, due to lack of time on Laura Stobie's part, only the accelerometer data was presented for analysis. There are three files approximately 2400 records long. (See Tables 15,17 and 19.) The flight computer uses an 8-bit word to record the sensor output counts which means that the output counts range from 0 to 255. The accelerometer gain factor equals 1,2, or 3 for full-scale ranges of 1,5, or 50. The input files were generated by Laura Stobie using a linear fit between counts with range factors, and

acceleration. Zero counts equal -1 mg, 255 counts equal +1 mg, and 127 counts equal 0 mg. Temperature effects were ignored. The code shown in Table 14 uses the same approach in calculating accelerometers from counts and gain factor and ignores temperature effects. The output files from this code are shown in Table 16,18, and 20. A comparison of these files with the original data used by Laura Stobie established that the code in Table 14 correctly calculates acceleration. The analyses of these output files appear in the next section of the report where they are used as input to the menu driven spreadsheet programs developed as part of this work.

Accelerometer Codes - The FORTRAN code is shown in Table 14. It was compiled with a Lahey 77® FORTRAN compiler, and run on an IBM® compatible PC. A version of this code can be found on the floppy disk attached to this report in a file named, A:\F77L\ACCLERB.FOR.

Table 14. FORTRAN code named ACCLERB.FOR Used to Convert Accelerometer Data with Simulated Flight Format into Engineering Units.

```
      PROGRAM ACCLERB                                                    ACB001
      CHARACTER*10 NULL                                                  ACB002
      OPEN(8,FILE='ACCLERB.INP',FORM='FORMATTED',STATUS='OLD')           ACB003
      OPEN(9,FILE='DAY3B.OUT',FORM='FORMATTED',STATUS='NEW')             ACB004
C                                                                        ACB005
C     This program takes the output counts and gain for the              ACB006
C     accelerometers from test data file, ACCLERB.INP, developed         ACB007
C     by Laura Stobie and calculates acceleration.                       ACB008
C                                                                        ACB009
C     Output from the program is acceleration in g's (ACCX,ACCY,ACCZ)    ACB010
C                                                                        ACB011
C     The output is in counts (XCOUNT,YCOUNT,ZCOUNT) Decimal = Gain      ACB012
C                                                                        ACB013
C      If gain factor = 1  Counts.1                                      ACB014
C      If gain factor = 2  Counts.2                                      ACB015
C      If gain factor = 3  Counts.3                                      ACB016
C                                                                        ACB017
C     This reads past header on ACCLERB.INP                              ACB018
C                                                                        ACB019
      DO 100 I=1,19                                                      ACB020
```

```
      READ(8,'(A10)') NULL                                              ACB021
  100 CONTINUE                                                          ACB022
C                                                                       ACB023
C     Reads following data from ACCLERB.INP                             ACB024
C                                                                       ACB025
C     IFRAME = Frame number (there are 8 data points per frame)         ACB026
C     IHR    = Number of hours in flight time                           ACB027
C     IMIN   = Number of minutes in flight time                         ACB028
C     ISEC   = Number of seconds in flight time                         ACB029
C     ICX    = Number of output counts from X-axis accelerometer        ACB030
C     IGX    = Gain of X-axis accelerometer (1 or 2 or 3)               ACB031
C     ICY    = Number of output counts from Y-axis accelerometer        ACB032
C     IGY    = Gain of Y-axis accelerometer (1 or 2 or 3)               ACB033
C     ICZ    = Number of output counts from Z-axis accelerometer        ACB034
C     IGZ    = Gain of Z-axis accelerometer (1 or 2 or 3)               ACB035
C                                                                       ACB036
  110 READ (8,2,END=120) IFRAME,IHR,IMIN,ISEC,ICX,IGX,ICY,IGY,ICZ,IGZ   ACB037
C                                                                       ACB038
C     Calculates time in seconds                                        ACB039
C                                                                       ACB040
      ITIME=ISEC+IMIN*60+IHR*3600                                       ACB041
C                                                                       ACB042
C     Calculates counts.gain for output to DAY3B.PRN                    ACB043
C                                                                       ACB044
      IF(IGX.EQ.1) XCOUNT=FLOAT(ICX)+.1                                 ACB045
      IF(IGX.EQ.2) XCOUNT=FLOAT(ICX)+.2                                 ACB046
      IF(IGX.EQ.3) XCOUNT=FLOAT(ICX)+.3                                 ACB047
      IF(IGY.EQ.1) YCOUNT=FLOAT(ICY)+.1                                 ACB048
      IF(IGY.EQ.2) YCOUNT=FLOAT(ICY)+.2                                 ACB049
      IF(IGY.EQ.3) YCOUNT=FLOAT(ICY)+.3                                 ACB050
      IF(IGZ.EQ.1) ZCOUNT=FLOAT(ICZ)+.1                                 ACB051
      IF(IGZ.EQ.2) ZCOUNT=FLOAT(ICZ)+.2                                 ACB052
      IF(IGZ.EQ.3) ZCOUNT=FLOAT(ICZ)+.3                                 ACB053
C                                                                       ACB054
C     Calculates acceleration with the following fit                    ACB055
C                                                                       ACB056
C     255 counts = +1 mg                                                ACB057
C     127 counts =  0 mg                                                ACB058
C       0 counts = -1 mg                                                ACB059
C                                                                       ACB060
C     Gain 1 multiplies counts by  1                                    ACB061
C     Gain 2 multiplies counts by  5                                    ACB062
C     Gain 3 multiplies counts by 50                                    ACB063
C                                                                       ACB064
      IF(IGX.EQ.1) ACCX=2.*FLOAT(ICX)/255.-1.                           ACB065
      IF(IGX.EQ.2) ACCX=(2.*FLOAT(ICX)/255.-1.)* 5.                     ACB066
      IF(IGX.EQ.3) ACCX=(2.*FLOAT(ICX)/255.-1.)* 50.                    ACB067
      IF(IGY.EQ.1) ACCY=2.*FLOAT(ICY)/255.-1.                           ACB068
      IF(IGY.EQ.2) ACCY=(2.*FLOAT(ICY)/255.-1.)* 5.                     ACB069
      IF(IGY.EQ.3) ACCY=(2.*FLOAT(ICY)/255.-1.)* 50.                    ACB070
      IF(IGZ.EQ.1) ACCZ=2.*FLOAT(ICZ)/255.-1.                           ACB071
      IF(IGZ.EQ.2) ACCZ=(2.*FLOAT(ICZ)/255.-1.)* 5.                     ACB072
      IF(IGZ.EQ.3) ACCZ=(2.*FLOAT(ICZ)/255.-1.)* 50.                    ACB073
C                                                                       ACB074
C     Writes output to DAY3B.PRN                                        ACB075
C                                                                       ACB076
      WRITE (9,3) ITIME,XCOUNT,ACCX,YCOUNT,ACCY,ZCOUNT,ACCZ             ACB077
      GO TO 110                                                         ACB078
    2 FORMAT(I8,I2,I3,I3,I4,I2,I4,I2,I4,I2)                             ACB079
    3 FORMAT(I6,F9.1,F9.4,F9.1,F9.4,F9.1,F9.4)                          ACB080
  120 CONTINUE                                                          ACB081
      STOP                                                              ACB082
      END                                                               ACB083
```

In the code shown in Table 14, time was converted to seconds using the equation in line ACB041. For output display convenience counts and gain factor were combined. The non-decimal part represents counts and the decimal part represents gain factor. (See lines ACB043 to ACB053.) A linear fit was used to

convert counts with gain factor to acceleration. The parameters for this fit appears in the comments. (See lines ACB055 to ACB073). The code shown in Table 14 requires an input file named ACCLERB.INP which contains: the simulated flight frame number; the time in hours, minutes, and seconds; the X, Y, Z accelerometer output in counts; and the gain factor for each of these axes. (See line ACB003 and ACB037.) A few lines at the beginning and at the end of the input file are displayed in Table 15. This file was developed by Tom Finley and Laura Stobie, and can be found in its entirety on the floppy disk in a file named, A:\F77L\ACCLERB.INP.

Table 15. Input File Named ACCLERB.INP Required for Code Shown in Table 14 Obtained from Tom Finley and Laura Stobie, IRD.

```
DATA STARTS ON RECORD 20                                          INC0001
                                                                  INC0002
KEY                                                               INC0003
                                                                  INC0004
A = Frame Number                                                  INC0005
B = Hours                                                         INC0006
C = Minutes                                                       INC0007
D = Seconds                                                       INC0008
E = X-Acc Output                                                  INC0009
F = X-Acc Gain                                                    INC0010
G = Y-Acc Output                                                  INC0011
H = Y-Acc Gain                                                    INC0012
I = Z-Acc Output                                                  INC0013
J = Z-Acc Gain                                                    INC0014
K = Acc Temp (Ordered X,Y,Z)                                      INC0015
                                                                  INC0016
                                                                  INC0017
   A B  C  D   E F   G H   I J   K                                INC0018
                                                                  INC0019
   1 0  0  1 127 1 127 1 127 1                                    INC0020
   1 0  0  1 127 1 127 1 127 1                                    INC0021
   1 0  0  1 127 1 127 1 127 1                                    INC0022
   1 0  0  1 127 1 127 1 127 1                                    INC0023
   1 0  0  1 127 1 127 1 127 1                                    INC0024
   1 0  0  1 127 1 127 1 127 1                                    INC0025
   1 0  0  1 127 1 127 1 127 1                                    INC0026
   1 0  0  1 127 1 127 1 127 1                                    INC0027
   2 0  0  2 127 1 127 1 127 1                                    INC0028
   2 0  0  2 127 1 127 1 127 1                                    INC0029

 2379 Records not printed

 299 0  4 59 149 3 253 2 127 1                                    INC2409
 299 0  4 59 149 3 253 2 127 1                                    INC2410
 299 0  4 59 149 3 254 2 127 1                                    INC2411
 300 0  5  0 149 3 254 2 127 1                                    INC2412
 300 0  5  0 149 3 254 2 127 1                                    INC2413
 300 0  5  0 149 3 254 2 127 1                                    INC2414
```

```
300 0  5  0 149 3 254 2 127 1                                    INC2415
300 0  5  0 149 3 254 2 127 1                                    INC2416
300 0  5  0 149 3 254 2 127 1                                    INC2417
300 0  5  0 149 3 140 3 127 1                                    INC2418
```

The code shown in Table 14 produces an output file (See line ACB004.) named DAY3B.OUT which contains the time in seconds, X-axis combined counts and gain factor, calculated X-axis acceleration, Y-axis combined counts and gain factor, calculated Y-axis acceleration, Z-axis combined counts and gain factor, and calculated Z-axis acceleration. A few lines at the beginning and end of the output file are displayed in Table 16 and all the lines can be found on the floppy disk in a file named A:\F77L\ACC\DAY3B.OUT. The file is in the A:\F77L\ACC\ directory since it is used in the menu spreadsheet program discussed in the following section of this report.

Table 16. Output File Named DAY3B.OUT Produced by Code Shown in Table 14.

```
  1   127.1  -0.0039   127.1  -0.0039   127.1  -0.0039          OUC0001
  1   127.1  -0.0039   127.1  -0.0039   127.1  -0.0039          OUC0002
  1   127.1  -0.0039   127.1  -0.0039   127.1  -0.0039          OUC0003
  1   127.1  -0.0039   127.1  -0.0039   127.1  -0.0039          OUC0004
  1   127.1  -0.0039   127.1  -0.0039   127.1  -0.0039          OUC0005
  1   127.1  -0.0039   127.1  -0.0039   127.1  -0.0039          OUC0006
  1   127.1  -0.0039   127.1  -0.0039   127.1  -0.0039          OUC0007
  1   127.1  -0.0039   127.1  -0.0039   127.1  -0.0039          OUC0008
  2   127.1  -0.0039   127.1  -0.0039   127.1  -0.0039          OUC0009
  2   127.1  -0.0039   127.1  -0.0039   127.1  -0.0039          OUC0010

  2371 Records not printed

299   149.3   8.4314   253.2   4.9216   127.1  -0.0039          OUC2390
299   149.3   8.4314   253.2   4.9216   127.1  -0.0039          OUC2391
299   149.3   8.4314   254.2   4.9608   127.1  -0.0039          OUC2392
300   149.3   8.4314   254.2   4.9608   127.1  -0.0039          OUC2393
300   149.3   8.4314   254.2   4.9608   127.1  -0.0039          OUC2394
300   149.3   8.4314   254.2   4.9608   127.1  -0.0039          OUC2395
300   149.3   8.4314   254.2   4.9608   127.1  -0.0039          OUC2396
300   149.3   8.4314   254.2   4.9608   127.1  -0.0039          OUC2397
300   149.3   8.4314   254.2   4.9608   127.1  -0.0039          OUC2398
300   149.3   8.4314   140.3   4.9020   127.1  -0.0039          OUC2399
```

Two additional input files are found in Tables 17 and 19. To produce the corresponding output files found in Tables 18 and 20, line ACB003 and ACB004

in the FORTRAN code (See Table 14.) must be modified to include the proper input and output file name. These changes were made, the code compiled and run. These files have the same format as that in Tables 15 and 16, respectively. A few lines at the beginning and end of the second input file are shown in Table 18 and all the lines can be found on the floppy disk in a file named A:\F77L\ACC\ACCLERB.IN1.

Table 17. Input File Named ACCLERB.IN1 Required for Code Shown in Table 14 Obtained from Tom Finley and Laura Stoble, IRD

```
DATA STARTS ON RECORD 20                                                IND0001
                                                                        IND0002
KEY                                                                     IND0003
                                                                        IND0004
A = Frame Number                                                        IND0005
B = Hours                                                               IND0006
C = Minutes                                                             IND0007
D = Seconds                                                             IND0008
E = X-Acc Output                                                        IND0009
F = X-Acc Gain                                                          IND0010
G = Y-Acc Output                                                        IND0011
H = Y-Acc Gain                                                          IND0012
I = Z-Acc Output                                                        IND0013
J = Z-Acc Gain                                                          IND0014
K = Temp (Ordered X,Y,Z)                                                IND0015
                                                                        IND0016
                                                                        IND0017
A   B  C  D   E F   G H I   J   K                                       IND0018
                                                                        IND0019
  1 0  0  1 170 1 176 1 129 1                                           IND0020
  1 0  0  1 170 1 176 1 129 1                                           IND0021
  1 0  0  1 170 1 176 1 129 1                                           IND0022
  1 0  0  1 170 1 176 1 129 1                                           IND0023
  1 0  0  1 170 1 176 1 129 1                                           IND0024
  1 0  0  1 170 1 176 1 129 1                                           IND0025
  1 0  0  1 170 1 176 1 129 1                                           IND0026
  1 0  0  1 170 1 176 1 129 1                                           IND0027
  2 0  0  2 170 1 176 1 129 1                                           IND0028
  2 0  0  2 170 1 176 1 129 1                                           IND0029

 2381 Records not printed

299 0  4 59 131 1 131 1 127 1                                           IND2411
300 0  5  0 131 1 131 1 127 1                                           IND2412
300 0  5  0 131 1 131 1 127 1                                           IND2413
300 0  5  0 131 1 131 1 127 1                                           IND2414
300 0  5  0 131 1 131 1 127 1                                           IND2415
300 0  5  0 131 1 131 1 127 1                                           IND2416
300 0  5  0 131 1 131 1 127 1                                           IND2417
300 0  5  0 131 1 131 1 127 1                                           IND2418
300 0  5  0 131 1 131 1 127 1                                           IND2419
301 0  5  1 131 1 131 1 127 1                                           IND2420
```

A few lines at the beginning and end of this output file are shown in Table 18. The output file can be found in its entirety on the floppy disk in a file named

A:\F77L\ACC\DAY5B.OUT. The file is in the A:\F77L\ACC\ directory since it is used in the menu program discussed in the following section of this report.

Table 18. Output File Named DAY5B.OUT Produced by Code Shown in Table 14.

1	170.1	0.3333	176.1	0.3804	129.1	0.0118	OUD0001
1	170.1	0.3333	176.1	0.3804	129.1	0.0118	OUD0002
1	170.1	0.3333	176.1	0.3804	129.1	0.0118	OUD0003
1	170.1	0.3333	176.1	0.3804	129.1	0.0118	OUD0004
1	170.1	0.3333	176.1	0.3804	129.1	0.0118	OUD0005
1	170.1	0.3333	176.1	0.3804	129.1	0.0118	OUD0006
1	170.1	0.3333	176.1	0.3804	129.1	0.0118	OUD0007
1	170.1	0.3333	176.1	0.3804	129.1	0.0118	OUD0008
2	170.1	0.3333	176.1	0.3804	129.1	0.0118	OUD0009
2	170.1	0.3333	176.1	0.3804	129.1	0.0118	OUD0010
2381 Records not printed							
299	131.1	0.0275	131.1	0.0275	127.1	-0.0039	OUD2392
300	131.1	0.0275	131.1	0.0275	127.1	-0.0039	OUD2393
300	131.1	0.0275	131.1	0.0275	127.1	-0.0039	OUD2394
300	131.1	0.0275	131.1	0.0275	127.1	-0.0039	OUD2395
300	131.1	0.0275	131.1	0.0275	127.1	-0.0039	OUD2396
300	131.1	0.0275	131.1	0.0275	127.1	-0.0039	OUD2397
300	131.1	0.0275	131.1	0.0275	127.1	-0.0039	OUD2398
300	131.1	0.0275	131.1	0.0275	127.1	-0.0039	OUD2399
300	131.1	0.0275	131.1	0.0275	127.1	-0.0039	OUD2400
301	131.1	0.0275	131.1	0.0275	127.1	-0.0039	OUD2401

A few lines at the beginning and end of this input file are shown in Table 19 and all the lines can be found on the floppy disk in a file named A:\F77L\ACC\ACCLERB.IN2. A few lines at the beginning and end of the third output file are shown in Table 20. The output file can be found in its entirety on the floppy disk in a file named A:\F77L\ACC\DAY13.OUT. The file is also in the A:\F77L\ACC\ directory since it is used in the menu spreadsheet program discussed in the following section of this report.

Table 19. Input File Named ACCLERB.IN2 Required for Code Shown in Table 14 Obtained from Tom Finley and Laura Stobie, IRD.

```
DATA STARTS ON RECORD 20                                                    INE0001
                                                                            INE0002
KEY                                                                         INE0003
                                                                            INE0004
A = Frame Number                                                            INE0005
B = Hours                                                                   INE0006
C = Minutes                                                                 INE0007
D = Seconds                                                                 INE0008
E = X-Acc Output                                                            INE0009
F = X-Acc Gain                                                              INE0010
G = Y-Acc Output                                                            INE0011
H = Y-Acc Gain                                                              INE0012
I = Z-Acc Output                                                            INE0013
J = Z-Acc Gain                                                              INE0014
K = Acc Temp (Ordered X,Y,Z)                                                INE0015
                                                                            INE0016
                                                                            INE0017
   A B  C  D   E F   G H   I J   K                                          INE0018
                                                                            INE0019
                                                                            INE0020
   1 0  0  1 127 1 127 1 127 1                                              INE0021
   1 0  0  1 127 1 127 1 127 1                                              INE0022
   1 0  0  1 127 1 127 1 127 1                                              INE0023
   1 0  0  1 127 1 127 1 127 1                                              INE0024
   1 0  0  1 127 1 127 1 127 1                                              INE0025
   1 0  0  1 127 1 127 1 127 1                                              INE0026
   1 0  0  1 127 1 127 1 127 1                                              INE0027
   1 0  0  1 127 1 127 1 127 1                                              INE0028
   2 0  0  2 127 1 127 1 127 1                                              INE0029
   2 0  0  2 127 1 127 1 127 1                                              INE0030

 2381 Records not printed

 299 0  4 59 165 1 174 1 130 1                                              INE2311
 300 0  5  0 165 1 174 1 130 1                                              INE2412
 300 0  5  0 165 1 174 1 130 1                                              INE2413
 300 0  5  0 165 1 174 1 130 1                                              INE2414
 300 0  5  0 165 1 174 1 130 1                                              INE2415
 300 0  5  0 165 1 174 1 130 1                                              INE2416
 300 0  5  0 165 1 174 1 130 1                                              INE2417
 300 0  5  0 165 1 174 1 130 1                                              INE2418
 300 0  5  0 165 1 174 1 130 1                                              INE2419
 301 0  5  1 165 1 174 1 130 1                                              INE2420
```

Table 20. Output File Named DAY13.OUT Produced by Code Shown in Table 14.

```
  1    127.1  -0.0039    127.1  -0.0039    127.1  -0.0039                  OUE0001
  1    127.1  -0.0039    127.1  -0.0039    127.1  -0.0039                  OUE0002
  1    127.1  -0.0039    127.1  -0.0039    127.1  -0.0039                  OUE0003
  1    127.1  -0.0039    127.1  -0.0039    127.1  -0.0039                  OUE0004
  1    127.1  -0.0039    127.1  -0.0039    127.1  -0.0039                  OUE0005
  1    127.1  -0.0039    127.1  -0.0039    127.1  -0.0039                  OUE0006
  1    127.1  -0.0039    127.1  -0.0039    127.1  -0.0039                  OUE0007
  1    127.1  -0.0039    127.1  -0.0039    127.1  -0.0039                  OUE0008
  2    127.1  -0.0039    127.1  -0.0039    127.1  -0.0039                  OUE0009
  2    127.1  -0.0039    127.1  -0.0039    127.1  -0.0039                  OUE0010

 2381 Records not printed

299    165.1   0.2941    174.1   0.3647    130.1   0.0196                  OUE2392
300    165.1   0.2941    174.1   0.3647    130.1   0.0196                  OUE2393
300    165.1   0.2941    174.1   0.3647    130.1   0.0196                  OUE2394
300    165.1   0.2941    174.1   0.3647    130.1   0.0196                  OUE2395
300    165.1   0.2941    174.1   0.3647    130.1   0.0196                  OUE2396
300    165.1   0.2941    174.1   0.3647    130.1   0.0196                  OUE2397
300    165.1   0.2941    174.1   0.3647    130.1   0.0196                  OUE2398
300    165.1   0.2941    174.1   0.3647    130.1   0.0196                  OUE2399
300    165.1   0.2941    174.1   0.3647    130.1   0.0196                  OUE2400
301    165.1   0.2941    174.1   0.3647    130.1   0.0196                  OUE2401
```

Future Work - The following tasks should be accomplished in the future to insure reliable data analysis. These recommendations are summarized in the final section of his report.

1. A final ASCII format for all the flight sensors must be developed and sent to GSFC for incorporation into their computer program which reads the raw data, votes, and converts the raw flight data into useful ASCII format.

2. The procedure, including the proposed format, should be tested by generating simulated raw flight data with the BCU and sending it to GSFC for conversion.

3. A procedure must be developed to calculate actual flight time for each data point. A hardware and software timing analysis will be required as part of this procedure.

4. Interpolation routines must be developed to allow all data to be correlated in flight time.

Demonstration Program - A menu driven spreadsheet program was developed and implemented to list and plot SEDS data in engineering units from the three sensor systems. A personalized 3-D color menu program was obtained as shareware from Tony Minichillo, 528 McRobert Ave., Toronto, Ontario, CANADA, M6E 4R4. It is strongly recommended that users of this menu driven spreadsheet program pay the $39 license fee. (See A:\3DMENU\3DMENU.DOC on the attached floppy disk for details.) The spreadsheet used in this program is QUATTRO PRO® which must be installed on your computer with a path to all directories. On the floppy disk attached to this report is an installation program called A:MENU.BAT. This batch file loads all the necessary files (with the exception of QUATTRO PRO®) to demonstrate the menu driven program. Running this batch file will create a directory named C:\F771\ and load files into this directory. If this directory exists on your computer (e.g. you have Lahey 77® FORTRAN) you might want to redo the batch file. The file name loaded in the macro in QUATTRO PRO® contains this directory as part of its name and must be changed also. A:MENU.BAT also creates a directory called C:\3DMENU\ and loads files into this directory. If you have a 3DMENU program installed on your computer it will over-write your file and destroy your menu. Copy your menu files to another directory, delete the files on C:\3DMENU\ and remove this directory before running A:MENU.BAT. In this program there is a main menu and two submenus. (See Fig. 7.) To install the menu program enter A:MENU. You should see the main SEDS Data Analysis menu on your screen. From this menu, choose

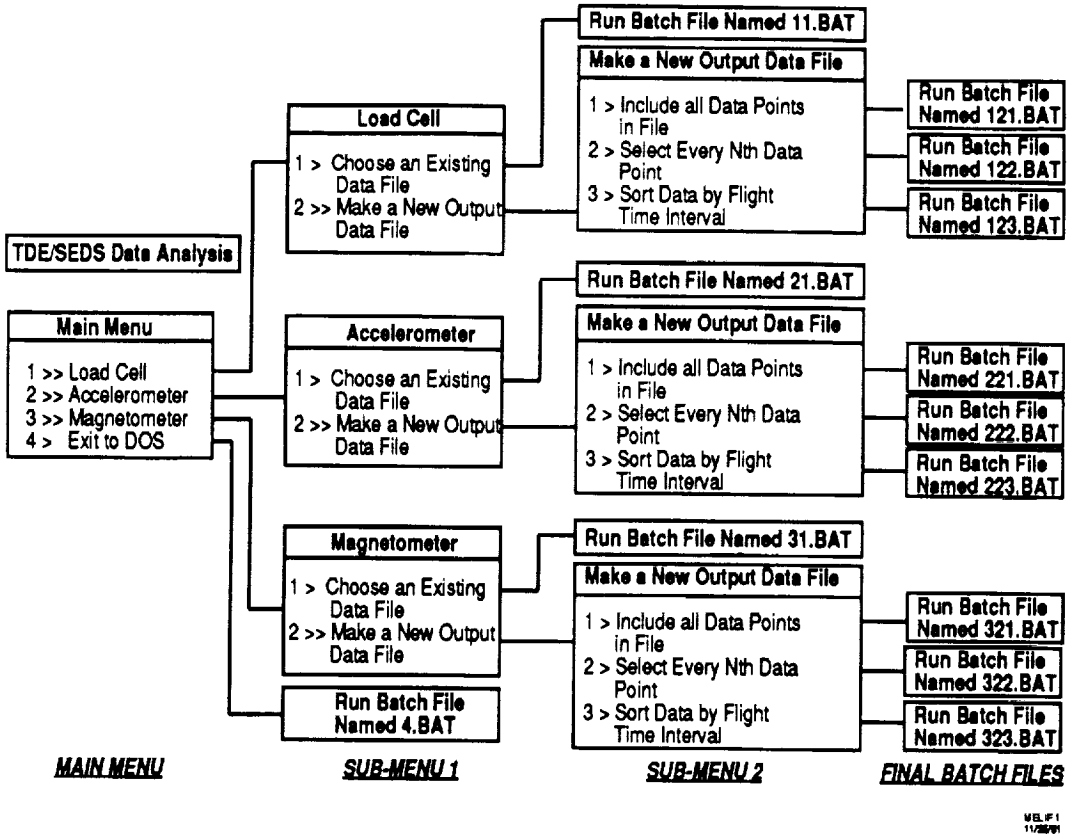

Fig. 7. Block Diagram of Menu Screen Display and Batch Files

the type (by instrument) of data you want to plot. You should now be at submenu 1. This submenu for all types of data allows two choices first, Choose an Existing Data File, and second, Make a New Output Data File. If you choose the second you should see submenu 2 which allows you to choose a number of options concerning the file you want to import into QUATTRO PRO®. These features are not presently implemented for any data type since this implementation requires large flight formatted file of actual or simulated data. This data is not presently available. A batch file will run to inform you that this feature is not implemented. The size of the flight data files for the load cell, accelerometer, and magnetometer data will be quite large. If the format in Table 15 is used, the file will have (assuming a 90 minute or 5400 second flight) approximately 43,000 records for

approximately 43,000 records for the load cell and accelerometer and 5400 records for the magnetometer. QUATTRO PRO® is limited to about 8192 records which either necessitates breaking up the files before-hand or using menu driven logic like that found in submenu 3. The menu method of breaking up the file allows you, in a convenient way, to choose your method without resorting to writing programs. If you choose Choose an Existing Data File you will find that data files do not presently exist for the load cell or magnetometer. A batch file will run to inform you of this fact. Press **ESC** until you return to the main menu and choose Accelerometer; at submenu 1 choose Choose an Existing Data File. Follow the instructions on the screen from which you can choose one of three existing data files. These are the files created in the previous section of this report. Make sure you enter the file name number either '1' or '2' or '3', and the data will be loaded into QUATTRO PRO. You can now list or plot any of this data. You might want to view a graph of all the imported data. Bring down the QUATTRO PRO® Graphics menu and select view. The plot shown on the screen should be identical to that shown in the appropriate figure discussed below in the Spreadsheet Results section.

Spreadsheet Results - Fig. 8, 9, and 10 are QUATTRO PRO® plots of the data in files A:\F77L\ACC\DAY3B.OUT, A:\F77L\ACC\DAY5B.OUT, and A:\F77L\ACC\DAY13.OUT, respectively. These plots are identical to those originally produced by Tom Finley and Laura Stobie and establish that the data have been converted to engineering units correctly and imported properly into

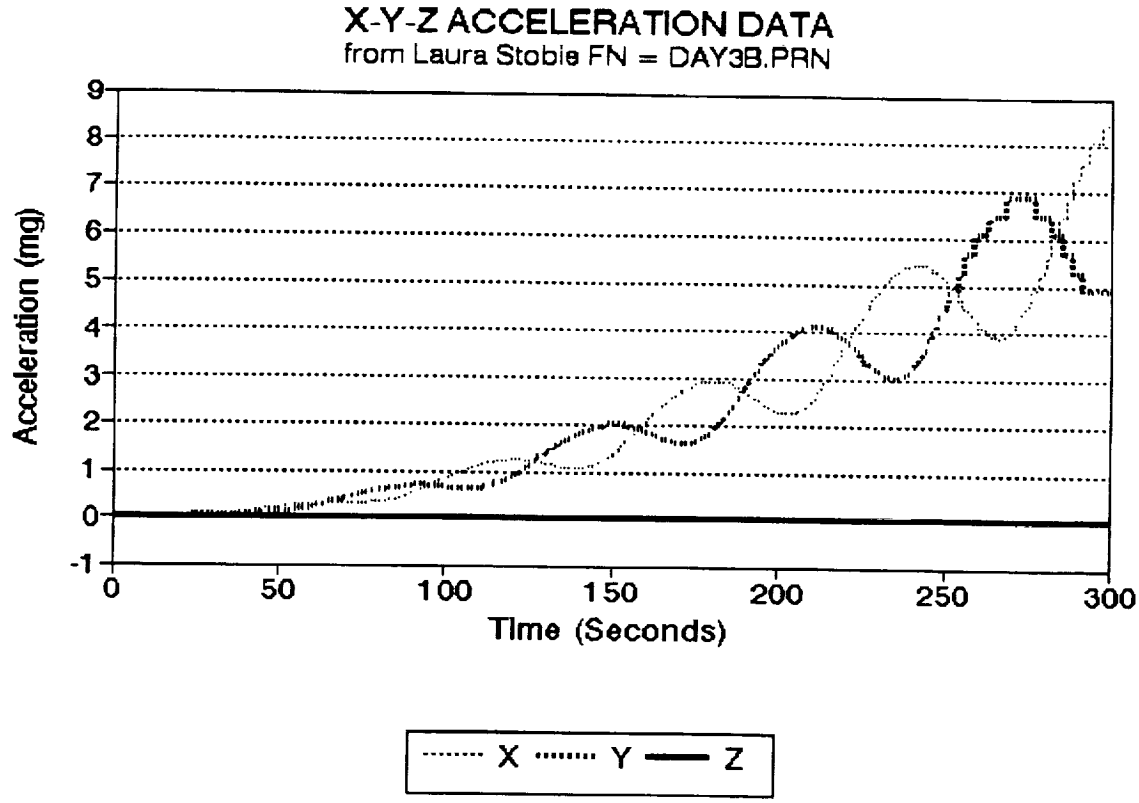

Fig. 8. QUATTRO PRO® Plot of Accelerometer Data on File Named DAY3B.PRN

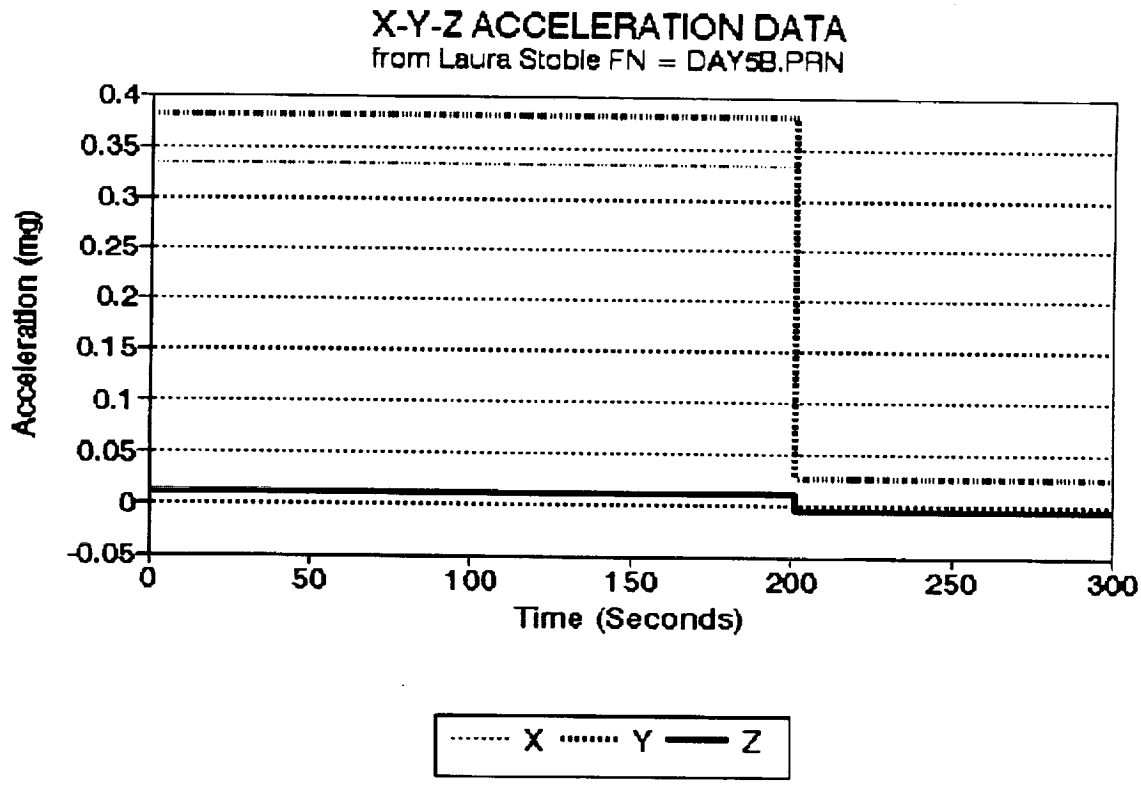

Fig. 9. QUATTRO PRO® Plot of Accelerometer Data on File Named DAY5B.PRN

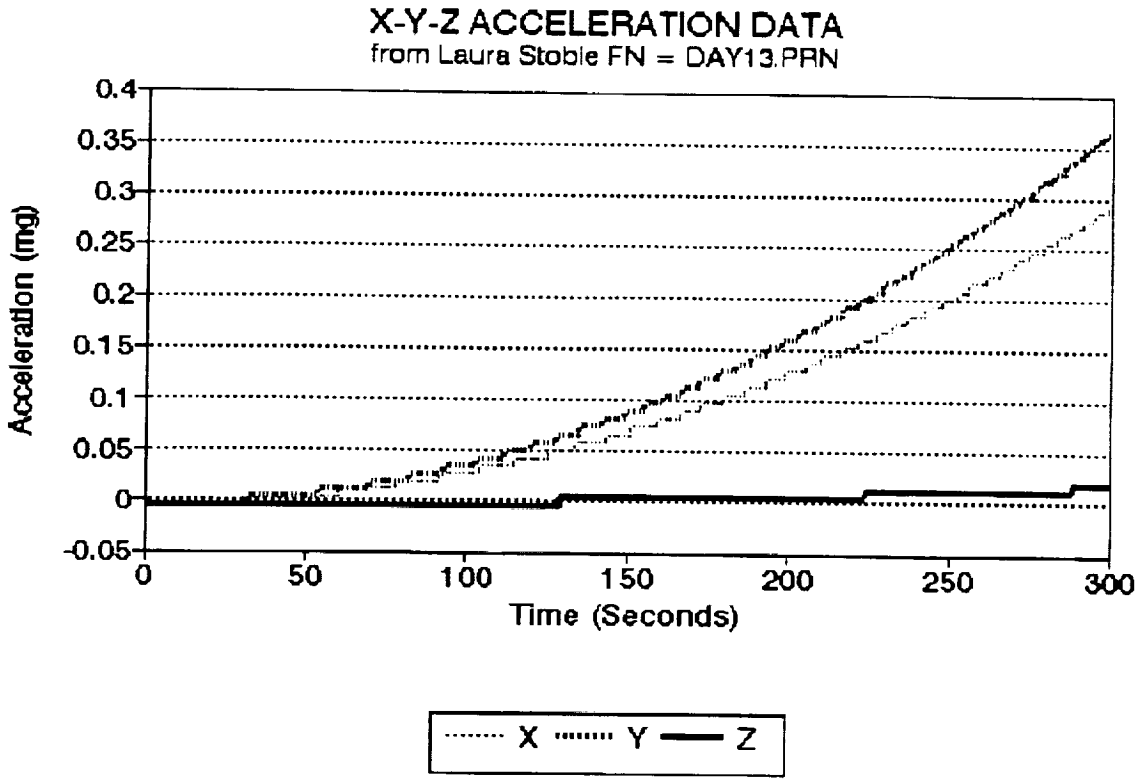

Fig. 10. QUATTRO PRO® Plot of Accelerometer Data on File Named DAY13.PRN

QUATTRO PRO®. It was planned to supply the dynamics user community with a complete set of the codes including the menu driven spreadsheet program and flight data files from which they could conveniently study end-mass dynamics.

Description of Menu Codes - The menu driven spreadsheet program requires a number of batch files (See in Fig. 7.). There is one batch file named A:\3DMENU\4.BAT in the main menu which changes the directory to C:\3DMENU\ and EXITS the 3DMENU program. There are three batch files in submenu 1 named A:\3DMENU\11.BAT, A:\3DMENU\21.BAT, and A:\3DMENU\31.BAT; and nine batch files in submenu 2 named

A:\3DMENU\121.BAT, A:\3DMENU\122.BAT, A:\3DMENU\123.BAT, A:\3DMENU\221.BAT, A:\3DMENU\222.BAT, A:\3DMENU\223.BAT, A:\3DMENU\321.BAT, A:\3DMENU\322.BAT, and A:\3DMENU\323.BAT. In submenu 2 A:\3DMENU\11.BAT and A:\3DMENU\31.BAT are not implemented; and none of the submenu 3 batch files are implemented. All eleven of these batch files are identical. (See floppy disk for listings.) They send a message to the screen informing the user that this feature is not implemented. The batch file named A:\3DMENU\21.BAT is implemented and performs the functions described in the previous Spreadsheet Results section. A listing of this file can be found in Table 21. This batch file needs to be upgraded to include tests for the existence of files before they are called.

Table 21. Batch File Named 21.BAT Used in Menu Driven Spreadsheet Program.

```
REM C:\3DMENU\21.BAT                                                    BAT001
REM                                                                     BAT002
REM LOADS TDE\SEDS ACCELERATION DATA INTO QPRO                          BAT003
REM                                                                     BAT004
ECHO OFF                                                                BAT005
REM                                                                     BAT006
REM CHANGES TO DRIVE AND DIRECTORY WHERE CODES RESIDE                   BAT007
REM                                                                     BAT008
c:                                                                      BAT009
cd\f771\acc                                                             BAT010
REM                                                                     BAT011
REM DELETES acclera.prn TO ALLOW IT TO BE OPENED AS NEW                 BAT012
REM                                                                     BAT013
del acclerb.prn                                                         BAT014
REM                                                                     BAT015
REM CHANGES SCREEN TO RED ON WHITE - THEN CLEARS SCREEN                 BAT016
REM type red_on.wht                                                     BAT017
cls                                                                     BAT018
REM                                                                     BAT019
REM DISPLAYS EXISTING DATA FILES ON SCREEN                              BAT020
REM      DETAILS IN fname_a.for                                         BAT021
REM                                                                     BAT022
fname_a                                                                 BAT023
REM                                                                     BAT024
REM TURNS BLINKER ON                                                    BAT025
REM                                                                     BAT026
REM type blinker.on                                                     BAT027
REM                                                                     BAT028
REM DISPLAYS PROMPT - READS USER'S CHOICE OF EXISTING DATA FILE         BAT029
REM    COPIES DATA TO acclerb.prn                                       BAT030
REM                                                                     BAT031
fname_b                                                                 BAT032
```

```
REM                                                                    BAT033
REM COPIES HEADER IN acclerb.wq1(QPRO FILE) TO tmporary.wq1            BAT034
REM   THIS COPY PROTECTS HEADER                                        BAT035
REM                                                                    BAT036
copy acclerb.wq1 tmporary.wq1                                          BAT037
REM                                                                    BAT038
REM RUNS QPRO WITH tmporary.wq1 AND MACRO \a                           BAT039
REM    tmporary.wq1 HAS THE HEADER - \a LOADS DATA FROM acclerb.prn    BAT040
REM                                                                    BAT041
q tmporary \a                                                          BAT042
REM                                                                    BAT043
REM TURNS BLINKER OF AND RETURNS TO MENU                               BAT044
REM                                                                    BAT045
REM type blinker.off                                                   BAT046
c:\3dmenu\menu                                                         BAT047
```

Most of the commands in the batch file named 21.BAT are self-explanatory; however, a few need further comments. In line BAT014 the file named ACCLERB.PRN is deleted since it is opened as a new file in the program in line BAT032. The files in lines BAT017, BAT027, and BAT046 have been commented out since they did not work on all computers when the demonstration program was tested. They have no effect on the other commands. The programs in lines BAT023 and BAT032 are FORTRAN codes which display the existing files on the screen and load the user chosen file into ACCLERB.PRN. Two FORTRAN codes are used to only blink the promp. (This feature is no longer active). These codes are listed in Table 22. The input file required by FNAME_A.FOR is listed in Table 23. In line BAT037 a QUATTRO PRO® file named ACCLERB.WQ1 is copied into TMPORARY.WQ1 to prevent the user from destroying it. This file contains the header, macro, and plotting instructions. QUATTRO PRO® is loaded in line BAT042 with its file named TMPORARY.WQ1 using its macro names \a (See Table 24.). Line BAT047 returns to the menu program at exit from QUATTRO PRO®.

Table 22. FORTRAN Files Named FNAME_A.FOR and FNAME_B.FOR Used in Batch File Named 21.BAT.

```
      PROGRAM FNAME_A
C
C     This code reads the names of existing TDE/SEDS acceleration data
C     files located in a file named FNAME_A.FIL - It is run from 21.BAT
C     in the 3dmenu program - Second Submenu - First Choice
C
      CHARACTER*12 FNAME1
      OPEN(8,FILE='FNAME_A.FIL',STATUS='OLD',FORM='FORMATTED')
C
C     Read the number of file names in FNAME_A.FIL
C
      READ(8,4) NREC
    4 FORMAT(I3)
C
C     Loads file name in FNAME1 and writes file name number and file name
C     to CON: - Write question input prompt to CON: - The READ from
C     CON: is in FNAME_B  after Blinker is turned on (see 21.BAT and
C     FNAME_B.FOR).
C
      DO 10 I=1,NREC
      READ(8,5) FNAME1
    5 FORMAT(12A)
      WRITE(5,6) I,FNAME1
    6 FORMAT(42X,I3,'. ',12A)
   10 CONTINUE
      WRITE(5,1)
    1 FORMAT(' Enter filename number as shown above   ')
      STOP
      END

      PROGRAM FNAME_B
C
C     This code continues the process started in FNAME_A. It
C     reads the names of existing TDE/SEDS acceleration data
C     files located in a file named FNAME_A.FIL  It is run
C     from 21.BAT in the 3dmenu program - Second Submenu -
C     First Choice
C
      CHARACTER*12 FNAME1(200)
      CHARACTER*80 C80
      OPEN(8,FILE='FNAME_A.FIL',STATUS='OLD',FORM='FORMATTED')
C
C     Read the number of file names in FNAME_A.FIL
C
      READ(8,4) NREC
    4 FORMAT(I3)
C
C     Load names in Character Array FNAME1
C
      DO 10 I=1,NREC
      READ(8,5) FNAME1(I)
    5 FORMAT(12A)
   10 CONTINUE
C
C     Write prompt to CON: should be blinking
C
      WRITE(5,1)
    1 FORMAT('                                          >')
C
C     Read user selected file name number
C
      READ(5,2) NFILE
    2 FORMAT(I3)
C
C     Open chosen file name and copy to ACCLERB.PRN
C
      OPEN(9,FILE=FNAME1(NFILE),STATUS='OLD',FORM='FORMATTED')
      OPEN(7,FILE='ACCLERB.PRN',STATUS='NEW',FORM='FORMATTED')
   20 READ(9,7,END=30) C80
      WRITE(7,7) C80
      GO TO 20
```

```
   30 CONTINUE
    7 FORMAT(80A)
C
C     Data in ACCLERB.PRN is that selected by user and will
C     be loaded into QPRO using macro \a (see 21.BAT)
C
      STOP
      END
```

Table 23. Input File Named FNAME_A.FIL Required for FORTRAN Codes Named FNAME_A.FOR and FNAME_B.FOR Listed in Table 22.

```
  3
DAY3B.OUT
DAY5B.OUT
DAY13.OUT
```

Table 24. Macro Named '\a' Used in Loading Data into QUATTRO PRO®.

```
~{GOTO}
a10
{/File;ImportNumbers}
{CLEAR}
C:\F77L\ACC\ACCLERB.PRN~
```

Future Work - Most of the logic has been developed for the menu driven spreadsheet program. There are a number of programming tasks remaining which should be done after the simulated flight data files are received from GSFC (See Future Work in ANALYSIS OF SIMULATED FLIGHT DATA section of this report.). Some of these tasks are listed below:

1. Batch files and their command files need to be written to implement the submenu 2 features, i.e. FORTRAN codes to sort the large flight data files to be imported into QUATTRO PRO®.
2. The sorted simulated flight data files can then be used to test the features in submenu 1.

3. The header and macro in QUATTRO PRO® should be modified to improve the QUATTRO PRO® presentation of the data and to import the data more efficiently.

4. Tests for file existence and for QUATTRO PRO® overflow should be included in all programs and batch files.

FUTURE WORK

Introduction - A complete data analysis plan is needed to insure that all data and computer codes necessary to analyze the SEDS end-mass data are available before flight. The work outlined in this report and the suggested future work could form the basis of this plan. A brief summary of future work is given in this section. This summary is taken from the Future Work and Considerations subsections throughout the text.

Flight Sensor System - Calibration data is required for all sensors with their electronics, the sensor diagnostics (e.g. sensor temperature, bridge voltage, etc.), and the A/D converter. As this data becomes available, the conversion programs must be modified to allow conversion to engineering units for the complete flight sensor systems. These modifications should not affect the basic structure of the present codes. A complete error analysis for each flight sensor system is required and the necessary measurement uncertainty data must be obtained. A computer program is required to obtain the time that each data point is taken. The actual flight time (our connection to the external world) is not contained on the flight frame and must be constructed from the data recording method. The three subsections summarized in this paragraph are **Calibration Considerations**, **Error Analysis Considerations**, and **Dynamic Data Considerations**. These subsections can be found at the end of the SEDS END-MASS FLIGHT SENSOR SYSTEM section of this report.

SEDS End-Mass Geometry - The following geometric properties of the sensors and the end-mass are required for the dynamics analyses of the end-mass: 1.) the position of each sensor with respect to each other and the end-mass, 2.) the sensor axes alignment in terms of the end-mass coordinate system, and 3.) the overall geometry of the end-mass including the cover, deployment and isolation system; 4.) the end-mass weight; 5.) the end-mass center of gravity; and 6.) the end-mass moments of inertia (mass and products). A computer program is needed to give the user the relationship of the sensor axes to the body axes (end-mass) or a coordinate transformation matrix must be developed for each sensor and should be included in the codes used to convert flight data to engineering data. The user would then be given the sensor outputs in body coordinates. The user also will need the data to reconstruct the overall body geometry, the end-mass weight, the mass moments and products of inertia. The subsection summarized in this paragraph can be found in the SEDS END-MASS GEOMETRY section, **Dynamics Data Analysis** subsection of this report.

Sensors Conversion Codes - The conversion codes for all three sensors should be tested to insure that they produce correct results for all possible flight cases. Testing procedures should be written and reviewed to insure that the conversion codes produce correct results. The temperature sensitivities for the load cell must be obtained and incorporated in the conversion codes. A temperature-time interpolation scheme must be developed since temperature measurements are not

taken at the same time or within the same time interval as the sensor outputs. A load cell output-time interpolation scheme must be developed since there is interaction between the load cell axes. Simultaneous outputs from all three axes are required to analyze the load cell data and these simultaneous outputs are not available on this mission. The output format from the conversion code must be determined and the codes modified to produce this output. Calibrations and temperature sensitivities of the magnetometer must be obtained and the codes modified to include this data. A magnetic field model for the orbital altitude range of the end-mass must be obtained and verified to allow comparisons with the magnetic field data obtained from the magnetometer. Computer programs need to be developed to perform these comparisons which are required to obtain end-mass dynamics and roll rate. There are three subsections, one for each sensor, summarized in this paragraph. They can be found in the ANALYSIS OF SENSOR CALIBRATION DATA section of this report. They are **Load Cell Future Work**, **Accelerometer Future Work**, and **Magnetometer Future Work**.

Flight Format - A final ASCII format for all the flight sensors must be developed and sent to GSFC for incorporation into their computer program which reads the raw flight data, votes on correctly transmitted data, averages the data, and converts the raw flight data into useful ASCII format. The procedure including the proposed format should be tested by generating simulated raw flight data with the BCU and sending it to GSFC for conversion. The subsection summarized in this

paragraph can be found in the FLIGHT FORMAT ANALYSIS section, **Future Work** subsection of this report.

Menu Driven Spreadsheet - There are a number of programming tasks remaining which should be done after the simulated flight data files are received from GSFC. (See Future Work in FLIGHT FORMAT ANALYSIS section of this report.) Batch files and their command files need to be written to implement the submenu 2 features shown in Fig. 7, i.e. FORTRAN codes to sort the large flight data files to be imported into QUATTRO PRO®. The sorted simulated flight data files can then be used to test the features in submenu 1. The header and macro in QUATTRO PRO® should be modified to improve the QUATTRO PRO® presentation of the data and to import the data more efficiently. Tests for file existence and for QUATTRO PRO® overflow should be included in all programs and batch files. The subsections summarized in this paragraph can be found in the MENU DRIVEN SPREADSHEET section, **Future Work** subsection of this report.

PART II

SHUTTLE BORNE TETHER SATELLITE SYSTEMS

Scope of the Work - There are 7 subtasks which are considered within the scope of work on this task. The first four were accomplished during the first year of the contractual period and these four subtasks are listed below:

1. Detailed definition of the previously identified data and measurement requirements.
2. Assessment of the current state of the art of instrumentation and identification of necessary instrument technology development.
3. Definition of instrumentation necessary to conduct the planned rarefied aerothermodynamics experiments.
4. Identify aspects of tether technology which may significantly reduce the cost and risk of space transportation operations.

Tether Review Article - This work was concerned mainly with Shuttle borne tether systems, measurement requirements, instrumentation assessment, aerothermodynamic instrumentation definition, and tether technology. A paper entitled "*Downward Deployed Tethered Satellite Systems, Measurement Techniques, and Instrumentation: A Review*" was prepared for the 4th International Tether Conference in Italy but the conference was canceled due to the Persian Gulf War. The paper was revised and submitted to the **Journal of Spacecraft and Rockets** as a review article. Further revisions were made to comply with the suggested changes of the referees and it was accepted for publication in the May/June 1992 issue of the **Journal of Spacecraft and Rockets**. The article as submitted is attached as Part II of this report.

DOWNWARD-DEPLOYED TETHERED SATELLITE SYSTEMS, MEASUREMENT TECHNIQUES, AND INSTRUMENTATION: A REVIEW

Kenneth G. Brown and Leonard T. Melfi, Jr.
Department of Chemistry and Biochemistry
Old Dominion University
Norfolk, VA 23529 USA

and

Billy T. Upchurch and George M. Wood, Jr.
Instrument Research Division
NASA Langley Research Center
Hampton, VA 23665 USA

Abstract

Data describing spacecraft atmospheric interactions in the lower terrestrial thermosphere (altitude range between 80 km and 200 km) are extremely limited due to the relative inaccessibility of this region to research vehicles. Atmospheric measurements in the lower thermosphere are sparse when compared to measurements on satellites at higher altitudes. Downward-deployed tethered satellites are being developed to allow access in a global sense to this important region of the atmosphere. This paper reviews: a number of Tether Satellite Systems emphasizing downward deployed systems to measure properties in the lower thermosphere; the physics and chemistry of the lower thermosphere; the interactions of the lower thermosphere with high velocity tethered satellites; and the performance capabilities of existing and

new instrumentation to measure atmospheric, aerodynamic, and aerothermodynamic properties which include radiative emission (glow), magnetism, and the distribution of the neutral gas, excited species, ions, and electrons. It is concluded that these tethered satellite systems, when implemented, offer a unique opportunity to investigate regions of the atmosphere previously inaccessible to conventional satellites.

Nomenclature

AE	Atmospheric Explorer
AFE	Aeroassist Flight Experiment
ASI	Agenzia Spaziale Italiana (Italian Space Agency)
AVM	Atmospheric Verification Mission
DE	Dynamic Explorer
HiRAP	High-Resolution Accelerometer Package
LDEF	Long Duration Exposure Facility
MSIS-86	Mass Spectrometer Incoherent Scatter Thermospheric Model
NASA	National Aeronautics and Space Administration
NASP	National Aero-Space Plane
SEDS	Small Expendable Deployer System
STS	Shuttle Transportation System
SUMS	Shuttle Upper Atmosphere Mass Spectrometer
STARFAC	Shuttle Tethered Aerothermodynamic Research Facility
T_e	Exospheric Temperature

TDE	Tether Dynamics Explorer
TSS	Tethered Satellite System

Introduction

NASA and ASI have developed and plan to fly TSS-1 in the second half of 1992. TSS-1 will be upward deployed and is designed to demonstrate tether dynamics and perform scientific studies on the electrodynamics of conducting tethers. The satellite and the Shuttle contain a large number of scientific instruments to perform these studies[1]. NASA is planning a number of follow-on downward-deployed tether satellite missions (See Fig. 1.) to study the aerodynamics and aerothermodynamics of hypersonic vehicles which traverse the lower thermosphere: 1.) The TSS-AVM[2] is proposed for flight in early 1995 and will be used to study aerodynamic forces, heating, and tether control at altitudes as low as 110 km. The satellite will be simple in design, not recoverable, and contain minimum instrumentation; 2.) TSS-2[3], proposed for flight in 1997, will be fully instrumented to characterize both vehicular aerodynamics and aerothermodynamics, and atmospheric structure. This satellite mission is presently being planned by both NASA and ASI; and 3.) STARFAC[4], proposed for flight late in this decade, will be fully instrumented and retrievable. This facility, which will fly at altitudes as low as 90 km, will be the first of a series of satellites whose shape and purpose will evolve to solve

specific practical aerothermodynamic problems of the 21st century.

In addition to these Shuttle based missions, NASA has scheduled in the latter half of 1992, a low cost tether mission[5] as a secondary payload on a Delta II launch vehicle. This mission will test SEDS which is being designed at NASA Marshall Space Flight Center. The TDE payload for this mission consists of instrumentation to study tether dynamics. NASA plans to develop and fly during the 1990's a series of these low cost flights to characterize tether dynamics, measure the environment around tethered satellites, and test instrumentation for future Shuttle based missions.

The Shuttle based downward deployed missions will be designed to obtain: atmospheric data in the lower thermosphere (altitude range between 80 and 200 km); aerodynamic data on the gas affected by spacecraft flying in this region; and aerothermodynamic data at the gas-spacecraft surface interface. This region of the atmosphere has not been studied in any detail since it is too high for balloons and research aircraft and too low for orbiting satellites. Sounding rockets have probed the region at limited locations and the AE satellite accessed this altitude range at perigee in its highly elliptical orbit. HiRAP[6], flown on-board the shuttle has been used to infer atmospheric density in this region during shuttle ascent and descent; and SUMS[7], another shuttle mounted experiment, has been used to measure species composition. AFE[8,9] is planned to fly in the mid 1990s and will probe this region on a limited basis. A summary[10] of the vehicular access to the lower thermosphere

can be found in Fig. 2. The data gathered on these vehicles are limited in a global sense to isolated points in time and space with the exception of the data gathered around perigee on the AE satellite. To emphasize the advantage of satellite measurement in studying the atmosphere, it is noted that more lower thermospheric data was gathered on the AE satellite missions than on all previous missions. Tethered satellites, which fly in the lower thermosphere, will give access in a global sense to this critical region of our atmosphere.

The purpose of this paper is to describe the measurements and instrumentation required to determine the structure of the lower thermosphere and its effects on high velocity vehicles like the Shuttle and the proposed NASP which traverse this little known region of our atmosphere. The structure of the lower thermosphere including the distribution of the neutral gas, ions, electrons, excited species and emissions (glow), and magnetism is discussed. Atmosphere-spacecraft interactions including the aerodynamics of a vehicle traversing this region of the atmosphere and aerothermodynamics at the spacecraft surface are also discussed. A review of the performance characteristics of existing flight qualified instruments is given and recommendations are made for the flight development of additional measurements techniques which are needed to improve accuracy, minimize weight and power, and simplify tether scientific instrumentation packages. This report concentrates on the definition of measurements and instrumentation for the TSS-AVM and TSS-2 Missions.

Atmosphere-Spacecraft Interactions

This section contains a brief review of 1.) the atmospheric properties of the lower thermosphere[11,12], 2.) The effects of the vehicle on the gas in its vicinity (Gas Phase Effects - Aerodynamics), and 3.) vehicular surface effects (Surface Effects - Aerothermodynamics). The atmospheric properties of the lower thermosphere are not well known in a global sense. Spacecraft are over-designed due to the lack of information and we are constantly being surprised by vehicular interactions with the atmosphere (i.e. O degradation, spacecraft glow, etc.).

Neutral Atmosphere. Below about 100 km the atmospheric gas consists mainly of molecular nitrogen and molecular oxygen, and its composition varies little in time and space. Above approximately 100 km the photo-dissociation of molecular oxygen and diffusion produce an atmosphere whose composition varies considerably in the vertical. Further, the atmospheric density, temperature, and composition varies with the solar cycle, solar activity, time of day, geomagnetism, and seasons. At a given latitude and longitude, the temperature increases with height and approaches T_e asymptotically. As an example, for medium sun conditions (T_e = 1000 K), the total density, temperature, and composition at 90 km is 7×10^{13} cm^{-3}, 188 K, and 0.78 N_2, 0.20 O_2, respectively and at 200 km is 7×10^{9} cm^{-3}, 885 K, and 0.40 N_2, 0.56 O,

respectively[13]. Atomic oxygen is a highly chemically reactive gas and is difficult to sample properly. N_2 is less reactive, stable and it remains a major constituent in the lower thermosphere. Atomic nitrogen, N is formed by processes other than photo-dissociation, has a peak density between 100 km and 200 km, and is a minor constituent with composition around 0.05. In addition to these static conditions, the upper atmosphere is dynamic; there are winds, gravity waves, and transport of gas in both the horizontal and vertical.

Ion Atmosphere. The three predominant positive ions in the lower thermosphere are O^+, NO^+, and O_2^+. O^+ is the predominant ion at altitudes above 200 km and becomes insignificant below 150 km. NO^+ is the largest ion constituent below 200 km. O_2^+ composition reaches its maximum at around 150 km but does not exceed the composition of NO^+. The absence of N_2^+ does not mean that this ion is not formed but that it disappears rapidly by dissociative recombination. Ions exist in the atmosphere in concentrations (10^5 cm^{-3}) much lower than neutral constituents; however, changes with time in these charged particles have been shown to have a major effect on the neutral atmosphere. Ions generally follow magnetic field lines in the upper part of the thermosphere and are swept along with the neutral gas at lower altitudes less than 130 km.

Atmospheric Electrons. The electron density increases with altitude from a few times 10^4 cm^{-3} at 100 km to approximately 10^6 cm^{-3} at 200 km. The lower thermosphere contains both the E layer (90 km to 160 km) and the F1 layer (above 160 km). The F2 peak is generally above 250 km. The electron density varies considerably throughout this region. This is particularly true in the E layer where transient abnormal ionization occurs on a more or less regular basis. Motions in the upper atmosphere can give rise to electric fields. Electrons and ions moving in response to these fields and the Earth's magnetic field form an electrical current. Examples of these currents are the large flows around the magnetic pole called the Birkeland current and an East-West current near the magnetic dip equator, at altitudes between 90 km and 130 km, known as the electrojet. These charged particle flows can transfer energy to the neutral gas causing heating and excitation.

Excited Species - Emissions. The presence of excited molecules is demonstrated quite graphically by observed emissions in the ultraviolet, visible, and near-infrared spectrum. These emissions are known as airglow and the aurora. Most of this glow originates in the lower thermosphere from collisional excitation and spontaneous decay of meta-stable states of the atmospheric gas. The gas is excited by photo-chemical processes which occur in the lower thermosphere. Most of the solar photon absorption occurs in the lower thermosphere which leads to heating, excitation, dissociation, and

ionization of the gas. A complicated combination of current flow, magnetic fields, and neutral winds are thought to contribute to the aurora which occurs at high latitudes and is much brighter than airglow. Interest in emissions has recently increased with the observation of spacecraft glow.

Magnetic Field. The terrestrial magnetic field can be divided into two components, the relatively constant field produced in regions interior to the Earth's surface and that produced by currents in the upper atmosphere. The interior field has a magnitude of about 30,000 nT, its horizontal component is in the direction of the magnetic north pole, its vertical component is zero at the magnetic dip equator and is maximum at the magnetic poles. The external component of the magnetic field has small regular variations due to lunar and solar tides (0.01) and larger variations (0.20) during magnetic storms. An electrojet has been used to explain anomalies at the magnetic equator. The interaction between neutrals, ions, and electrons in the presence of the Earth's magnetic field outlines the importance of studying the atmosphere as a whole. In-situ measurements on tethered satellites offer this opportunity.

Gas Phase Effects - Aerodynamics. A high velocity vehicle traveling through the atmosphere interacts with the gas producing a gas build up in front of the vehicle and a reduced gas density behind the vehicle. This effect is demonstrated in Fig. 3 which shows lines of constant number density

normalized to freestream density[14] for a sphere traveling at orbital velocity at an altitude of 130 km as calculated with the Direct Simulation Monte Carlo method[15]. Just in front of the vehicle the density is a factor of 12 times the freestream (not shown in Fig. 1), decreases with distance from the body, and approaches the freestream density at about a satellite body diameter in the forward direction. The density behind the vehicle is reduced substantially reaching a value less than 0.05 times the freestream density.

Below 130 km, the density of the gas near the surface increases to the extent that freestream molecules can not traverse this gas without having many gas-gas collisions which heat the gas, and cause excitation and dissociation of molecules. These effects are summarized[16] in Fig. 4 which shows typical flight paths for high and low lift vehicles plotted as a function of both altitude (atmospheric density) and spacecraft velocity. The high lift entry trajectory is typical of the next generation Shuttle and the low lift entry trajectory is typical of NASP. The flight path of the present Shuttle lies between the high lift and low lift curves. Superimposed on this plot are percent dissociation and vibrational excitation for molecular nitrogen and oxygen. All of the effects to the left of the flight path curve are possible. As an example, at 90 km and orbital velocity (approx. 8 km/s) a large fraction of N_2 is dissociated, all of O_2 is dissociated, and vibrational excitation is possible for most of the molecular atmospheric species.

The high velocity vehicle also produces a flow of charged particles, ions

and electrons, in its vicinity and onto its surfaces. This current, in the presence of the Earth's magnetic field, can substantially change the local electric field, cause spacecraft charging, and further complicate the plasma near the vehicle[17]. The plasma which can be substantial in the lower thermosphere can also affect the local magnetic field near the vehicle. At altitudes below 130 km, the plasma around the vehicle is dense enough to cause attenuation of radio communications. The plasma is caused by the ion sheath found around hypervelocity vehicles.

A complex combination of gas-surface collisions and chemical processes is known to excite molecules in the gas near vehicle surfaces. The decay of these excited states produces light emissions which have been observed in the vicinity of the Shuttle vertical fin and on other orbital spacecraft[18]. These emissions have been observed in the ultraviolet, visible, and near infrared. The likely excited molecular species include OH, CO, NO and NO_2. For the Shuttle glow the most intense region occurs in the red (approx. 700 nm).

The distribution of the: neutral gas density, its temperature, and composition; ion density, its energy, and composition; electron density and energy; excited molecules and their photon emissions; and the electric and magnetic fields are all substantially changed near the spacecraft. The characterization of these changes and the extent to which they extend into the local atmosphere should be thoroughly investigated.

Surface Effects - Aerothermodynamics. The effects on spacecraft surfaces come

from the interaction of the high velocity gas, ions, and electrons with the surfaces. The complex molecular interactions lead to surface heating, gas adsorption and desorption, excitation, and chemical changes of the gas on surfaces. These effects lead directly to degradation of most surface materials particularly in the presence of atmospheric atomic oxygen. Ions and electrons interacting with the vehicle cause surface charging[19] which can lead to currents through the spacecraft, discharges, interference with and damage to sensitive instruments and electronic packages.

Above 130 km, the gas arriving at the surface is substantially unaffected freestream gas. The collision frequency in the higher density gas layer around the vehicle is low enough that the freestream gas is not affected before surface collisions. Heating rates are low enough that they do not drive vehicle thermal design. Collisions with the surface have enough energy to excite and dissociate freestream molecules. The residence times on the surface are large enough to allow chemistry to occur. Indeed the surface can act as a third body allowing chemical reactions to occur which are not probable in the gas. Chemical combinations of O and N from the gas phase and C (from the material) and H (from water) from the surface will exist on the surface and can desorb into the gas phase. These chemical effects manifest themselves in two important problems faced by spacecraft designers, spacecraft glow[18] and O degradation of surface materials[20].

Below 130 km, a substantial buildup of gas occurs at the surface in the

flow direction. As a result the freestream gas can not reach the vehicle surface without colliding with other gas phase molecules releasing energy to these molecules which results in significant heating of the gas. This hot gas transfers its energy to the surface, heating the surface to high temperatures. N_2 and O_2 dissociate in the gas, arrive at the surface as atoms, and can combine with themselves, other gas phase atoms adsorbed on the surface, and other surface species such as C (from the material) and H (from water). This molecular recombination can be a major surface heating mechanism. An ion sheath develops in flow around the vehicle at altitudes between 95 km and 125 km which causes surface charging and radio communication problems. These heating, charging, and communication effects must be considered in vehicle design.

Instrumentation

The purposes of the downward-deployed tethered missions are to determine: 1.) atmospheric and aerodynamic effects in the vicinity of the tethered satellite and aerothermodynamic effects on its surface; and 2.) the dynamics of the tether and its end-mass, the satellite. This paper will concentrate on the former. Instrumentation (accelerometers, tensiometers, etc.) and data analysis for tether dynamics are treated elsewhere[21,22] and are not considered within the scope of this paper. It should be noted that the analysis of this dynamic

data gives satellite drag which can be used to infer atmospheric density and temperature. (This technique is not discussed in this paper). These inferences could be useful in interpreting atmospheric, aerodynamic, and aerothermodynamic data .

Both in-situ and remote sensing techniques can be applied to measuring flow field and surface parameters on and around tethered satellites. To completely describe both freestream atmospheric and vehicle disturbed parameters, sampling should be made throughout the flow field up to at least a satellite body diameter away from the surface (See Fig. 3.). For the in-situ measurements this will probably require sampling booms. Measurements should also be made at a number of points on the satellite surface to characterize the effects of gas surface interactions on the spacecraft. No attempt will be made to give experiment design considerations. This paper is limited to the discussion of existing instrumentation which could form the basis for future experiment design. Instrumentation includes: mass spectrometers and other density measuring devices; plasma devices such as Langmuir probes and other electrostatic analyzers; optical spectrophotometers; magnetometers; and surface devices such as thermocouples, heat transfer transducers, O flux density sensors, etc..

Mass Spectrometers - Other Density Sensors. A number of flight mass spectrometers have been flown to measure constituent density in the lower

thermosphere. These include the open source neutral mass spectrometer flown on the Atmospheric Explorer Satellite[23] and rocket probe mass spectrometers[24] flown during the Energy Budget Campaign. There have been a number of review articles[25,26] on the Atmospheric Explorer and Energy Budget Campaign from which a more detailed reference list can be obtained. Recently, a rocket probe experiment[27] to measure N_2 and Ar was reported which covered the altitude range between 90 km and 130 km. Typically, satellite and rocket probe mass spectrometers weigh less than 10 kg and require less than 15 W average operating power.

These flight instruments offer a base from which aerothermodynamic and atmospheric experiments on tethered satellites can be developed. Aerothermodynamic experiments are different from atmospheric science experiments in the sense that a distribution of the flow field parameters is needed for each time and space point as opposed to a single atmospheric data point. (In the atmospheric science case, the effects of the vehicle are considered a data analysis complication.) To measure density distribution, an articulated sampling probe (arm), designed to minimize gas flow effects, is required to survey the entire volume around the spacecraft. For spacecraft which have attitude control systems the survey may be made with a boom that is not articulated but is extendable and retractable. For the spacecraft flowfield results given in Fig. 3, a sampling probe with a maximum length of the order of (exceeding) a body diameter (where the ratio of effected gas density

to freestream gas density, in the forward direction, is less than 2) would allow density measurement to be made throughout most of the disturbed gas and at the boom's full extent would allow the accurate measurement of freestream density. Another consideration is the high density at altitudes below 150 km which will require gas reduction methods as part of the mass spectrometer system. Also, O and O_2 (major atmospheric constituents) are highly chemically reactive and can cause degradation of the hot cathode in the mass spectrometer ion source (low emittance/power coated cathode will be required). These highly reactive gases are difficult to accurately measure since they recombine and form molecules that are associated more with gas-surface interactions than gas phase density. Proper sampling of this highly reactive gas near the satellite is required. Techniques used in the past include: transparent semi-nude ion sources imbedded in the flow, cryogenic cooling of the ion source and satellite surfaces, and molecular beam techniques. Ion gauges have also been used to measure total density in the lower thermosphere; however, these gauges are gas composition sensitive and their use is generally restricted to altitudes below 110 km where the composition is less variable. These gauges are small in physical size, are less complicated, can be operated at much higher density, and require much less power than mass spectrometers. Ion gauges were flown during the Energy Budget Campaign[26] and one is proposed to measure satellite orientation on tethered satellites[28]. Typical weight for flight ion gauges are 1 kg and require less than 2 W average

operating power.

Recently, an ion trap mass spectrometer[29] which is similar to ion gauge in size and complexity has become commercially available. (See Fig. 5.) Ions are trapped in the ion source by a quadrupole electric field and extracted for analysis by mass. This mass spectrometer[30] is simple to construct, is small in physical size, has high mass resolution (75), and can be constructed with transparent grids to operate imbedded in the flow to altitudes as low as 105 km[31]. The flight development of this instrument should be considered for density measurements on tethered satellites. Estimated weight and power consumption is less than 2 kg and 2 W, respectively.

Electron beam fluorescence[32] could be used to measure or infer the density distribution in the flow field near tethered satellites. The application of this technique should be thoroughly investigated since the need for instruments on probes is eliminated and a spectrophotometer which is needed to measure the fluorescence will probably be included in the spacecraft instrumentation package to measure vehicle and atmospheric glow. (See Optical Spectrophotometers section of this paper.)

Plasma Instrumentation. There are a number of instruments which have flown on both satellites (Atmospheric Explorer and Dynamic Explorer) and rocket probes (Project Condor) to study ion and electron concentrations and electric fields. Further, TSS-1 contains several of these instruments[33] to determine

electric field structure, and charged particle constituent density and temperature in the vicinity of the satellite. The instruments on these missions include: ion mass spectrometers to measure ion constituent density; retarding potential analyzers to measure total ion and electron density and energy distribution; and multiple probe systems to measure electron density distribution (Langmuir); and electric fields. Again, it should be noted that the distribution of parameters in the vicinity of the satellite is required to understand the complex nature of the ion and electron flow in the presence of charged surfaces, and the ambient and disturbed electric and magnetic field.

Ion mass spectrometers have been flown on both satellites[34] and rocket probes[35,36,37] to measure ion constituent density. The previously mentioned review articles[25,26] also give a more complete reference list for ion mass spectrometers. An ion mass spectrometer is basically a neutral mass spectrometer without an ion source. Most of the comments on neutral mass spectrometers (See Mass Spectrometers - Other Density Sensors section of this paper.) apply to ion mass spectrometers. An exception is that sampling problems are less complicated since ambient ions can be controlled with electric fields prior to analysis. The ion trap mass spectrometer (previously mentioned) should be investigated for possible use as an ion constituent density measurement device. It should be noted that other plasma devices discussed in the rest of this section are total ion detectors and can not discriminate ion species.

Retarding potential analyzers have been used in flight[38,39] to measure total ion and electron density and energy distribution. This device is basically a gridded cylindrical cavity, is simple to construct, is small in physical size and requires minimum operating power. Retarding potential analyzers have been used in conjunction with mass spectrometers to separate the high velocity freestream gas from lower velocity surface collided gas and on ion mass spectrometers to obtain constituent ion energy distributions[40].

Probes on booms, to minimize the effect of central body potential, have had extensive use in space flight. On DE Langmuir probes routinely provided fast response (2 sample/second) electron density and temperature measurements[41]. Further, the frequency and current of an extended antenna, as used on project Condor[42], were measured from which electron density was derived. The electric field instrument[43] on DE, which consisted of symmetric double probes mounted at the end of booms provided data on both the dc and ac electric fields. An ion drift meter[44] on DE gave the east-west components of total ion drift velocity. These and other electrostatic devices as a class are in general relatively simple, are small in physical size and weight, and require low operating power.

Optical Spectrophotometers. Most spectrophotometric measurements that have been made with instrumentation on-board rockets or satellites have been intended for long range sensing of emissions from atmospheric species[45,46]

to study airglow and the aurora. One interesting exception is an experiment containing a UV monochromator with a light source mounted on a boom extending from a rocket. This experiment, designed to measure O atom density by resonance fluorescence, has been flown on several rockets[47]. The data[48] from these flights are found to be in good agreement with MSIS-86[49]. A newly proposed experiment involves a Ebert-Fastie spectrophotometer (See Fig. 6.) which is being developed for AFE[50].This instrument has a 0.6 nm resolution, weighs about 3.5 kg and requires less than 30 W of operating power, and is designed to measure the total radiation produced by the vehicle in the visible and ultraviolet regions of the spectrum. No attempt is being made in the AFE flight to perform a depth profile of the radiation field nor is the resolving power of the instrument high enough to completely identify the excited species produced in the atmosphere and by the interaction of the vehicle with atmospheric gases.

Spectrophotometric observations of excited species produced by the interaction of a vehicle with atmospheric gases have been made on both the AE satellites[51] and the Shuttle[18] (the Shuttle glow phenomenon). In each case the resolution and spectral range of the instruments was not sufficient to conclusively identify the species producing the emission (The highest resolution was 3.4 nm on the Shuttle.). The resolution and spectral range available with the Ebert-Fastie spectrophotometer described above would substantially improve these measurements but it does not have the resolution to fully

identify the species produced both during satellite descent and orbit. There are small, lightweight spectrophotometers that are commercially available with high resolution (0.06 nm) in the required spectral range. The flight development of these spectrophotometers would allow identification of the species that are producing the light emission as well as the energy state from which the light is being emitted. These measurements would allow the extent of energy accommodation on the surface, the chemical reactions that take place on the surface, and the overall energetics of the surface-gas interactions to be determined.

Magnetometers. Magnetometers have been flown from the beginning of the space age to measure the terrestrial magnetic field in orbit. A number of satellites (DE-2[52], S3-3[53], and AE-C[54]) have contained magnetic field measuring instrumentation. The Magsat satellite was dedicated to sophisticated magnetic field measurements and successfully measured the magnetic field in the upper atmosphere. Magsat instrumentation[55,56,57] included both absolute sensors which sense the magnetic field effects on the frequency of atomic transitions (Zeeman effect) and relative measurement devices which use multiple nulled reference coils to give magnetic field magnitude and direction.

These flight magnetometers offer a base[58] from which directional magnetic field measurements can be made on tethered satellites in the lower

thermosphere. Deep in the ionosphere, the magnetic field in the vicinity of the satellite can be driven by atmospheric currents and vehicular effects due to the flow of ions and electrons around the spacecraft. The separation of these magnetic field effects into their components using both instrument and data analysis techniques should be a major consideration for magnetic instrumentation on low altitude tethered satellites. To properly analyze magnetic field data the satellite position must be accurately known, the electric field (ion and electron concentrations) in the vicinity of the spacecraft must be measured, and the satellite magnetic signature must be known or nulled during testing and calibration. Magnetic field measurements should be made throughout the plasma sheath near the vehicle. The extent of the disturbed magnetic field can be substantial, as an example, the Shuttle plasma sheath is estimated to extend to 400 m forward, 1.5 km aft, and 0.5 km normal to the flow.

Surface Instrumentation. Instrumentation to measure the effects on surfaces imbedded in a high velocity, chemically reactive gas which contains free ions and electrons can be divided into a number of classes. These include sensors and measurement techniques to determine the following: surface temperature, heat transfer, and pressure; gas adsorption on surfaces, chemistry with other gas molecules and surface material, and desorption from the surface; and surface charging.

Thermocouples and heat transfer transducers have found extensive use in measuring surface temperature and the transfer of energy from the gas to the spacecraft surface and are included into the design of most spacecraft. Fig. 7 shows proposed locations for heat transfer transducers on the TSS-AVM mission being studied by NASA and Martin Marietta[2]. These devices will be used to determine surface heat transfer distribution at altitudes as low as 110 km. For an altitude of 120 km, the surface temperature can reach values as high as 700 K at the stagnation point. (See Fig. 7 in Ref. 2). The surface temperature distribution can also be used to determine satellite orientation. Orientation sensitive high pressure ion gauges[28] mounted on the surface at a number of locations have been proposed to measure surface pressure and to give inputs to vehicle attitude control systems.For the most part gas adsorption and desorption and gas chemistry on spacecraft surfaces have been inferred from other measurements such as the interpretation of the source of shuttle glow[18] and the modeling of temperature and heat flow measurements upon shuttle reentry[59]. Direct measurement of the net result of this chemistry has been obtained from materials exposed to space environment in the shuttle bay[60] and samples retrieved from LDEF[61]. Velocity distributions of oxygen atoms were also estimated by examining etching patterns of surfaces exposed to the flow on STS-8[62]. The above measurements depended upon retrieving the experiment and estimating the O flux density which was not measured. Recent development of small, lightweight, low power O flux density

sensors (See Fig. 8.)[63] will allow O flux density on the satellite and tether surfaces to be measured directly. Sputtering of surface material by ambient ions has been observed[34] in flight mass spectrometers and should be investigated as a possible inflight surface analysis technique.Surface charging of the satellite affects the plasma measurements that have been discussed and influences the surface chemistry. Both the magnitude of the surface charge and its sign must be measured. The negative potential of rocket payloads has been determined by electrostatic analyzers which measured the cutoff of the ion energy spectra of ions interacting with the rocket surfaces[64]. A similar effect for electrons does not seem to exist either on rocket payloads[65] or on the shuttle[66]. A number of the electrostatic analyzers outlined in the Plasma Instrumentation Section of this paper could be used (modified) to measure surface charge.

References

1. Penzo, P. A., and Ammann, P. W., Tethers in Space Handbook, 2nd ed., NASA Headquarters, Washington, DC, May, 1989.

2. Wood, G. M., Stuart, T., Crouch, D., Melfi, L. T., and Brown, K. G., "Atmospheric verification Mission for the TSS/STARFAC Tethered Satellites," AIAA Paper 91-0534, Jan., 1991.

3. Wood, G. M., Siemers, P. M., Squires, R. K., Wolf, H., Carlomagno, G. M., and de Luca, L., "Downward-Deployed Tethered Platforms for High-Enthalpy Aerothermodynamic Research," *Journal Spacecraft and Rockets*, Vol. 27, March, 1990, pp. 216-221.

4. Siemers, P. M., Wood G. M., Wolf, H., Flanagan, P. F., and Henry, M. W., "The Definition of the Shuttle Tethered Aerothermodynamics Research Facility," AIAA Paper 85-1794, Aug., 1985.

5. DeLoach, R., Diamond, J., Finley, T., and Rhew, R., "End-Mass Instrumentation for the First SEDS/Delta-II Mission," AIAA Paper 90-0537, Jan., 1990.

6. Blanchard, R. C., Hendrix, M. K., Fox, J. C., Thomas, D. J., and Nicholson, J. Y., "Orbital Acceleration Research Experiment," *Journal Spacecraft and Rockets*, Vol. 24, Nov., 1987, pp. 504-511.

7. Blanchard, R. C., Duckett, R. J., and Hinson, E. W. J., "The Shuttle Upper Atmosphere Mass Spectrometer Experiment," *Journal Spacecraft and Rockets*, Vol. 21, Mar., 1984, pp. 202-208.

8. Jones, J. J., "The Rationale for an Aeroassist Flight Experiment," AIAA Paper

87-1508, June, 1987.

9. Blanchard, R. C., "Rarefied-Flow Aerodynamics Measurement Experiment on the Aeroassist Flight Experiment," AIAA Paper 89-0636, Jan., 1989.

10. This figure is an updated version of the figure found in: Anderson, J. L., Tethered Satellite System 2, A Planning Guide, NASA Headquarters, Washington, DC, May, 1989.

11. Craig, R. A., The Upper Atmosphere: Meteorology and Physics, Academic Press, New York, 1965, pp 235-274.

12. Heicklen, J., Atmospheric Chemistry, Academic Press, New York, 1976, pp. 1-44.

13. Jacchia, L. G., "Thermospheric Temperature, Density, and Composition: New Models," Smithsonian Astrophysical Observatory Special Report 375, Cambridge, MA, March, 1977.

14. Wood G. M., Jr., Wilmoth, R. G., Carlomagno, G. M., and de Luca, L., "Proposed Aerothermodynamic Experiments in Transition Flow Using the NASA/ASI Tethered Satellite System-2," AIAA Paper 90-0536, Jan., 1990.

15. Bird, G. A., "Monte-Carlo Simulation in an Engineering Context," in AIAA Progress in Astronautics and Aeronautics: Rarefied Gas Dynamics, ed. Sam S. Fisher, Vol. 74, Part 1, 1981, pp. 239-255.

16. Anderson, J. D., Jr., Hypersonic and High Temperature Gas Dynamics, McGraw-Hill, New York, 1989, p. 375.

17. Webster, W. J., Jr., "Engineering Tethered Payloads for Magnetic and

Plasma Observations in Low Orbit," *Journal Spacecraft and Rockets*, Vol. 26, March, 1989, pp. 80-84.

18. Mende, S. B., Swenson, G. R., and LLewellyn, E. J., "Ram Glow: Interaction of Space Vehicles with the Natural Atmosphere," *Advances in Space Research*, Vol. 8, No. 1, 1988, pp. 229-241.

19. Grard, R., Knott, K., and Pedersen, "Spacecraft Charging Effects," *Space Science Reviews*, Vol. 34, No. 3, 1983, pp. 289-304.

20. Marinelli, W. J., "Collisional Quenching of Atoms and Molecules on Spacecraft Thermal Protection Surfaces," AIAA Paper 88-2667, June, 1988.

21. Deloach, R., "Uses of Tethered Atmospheric Research Probes," AIAA Paper 91-0533, Jan., 1991.

22. Ioup, G. E., Ioup, J. W., Amini, A., Rayborn, G. H., Wong, D., and Wood, G. M., "Enhanced Data from Analytical Instrumentation by Deconvolution of Periodically Sampled Signals," Computers and Experiments in Stress Analysis, (eds.G. M. Carlomagno and Brebbia, C. A., Springer-Verlag, New York), 1989, pp. 449-460.

23. Nier, A. O., Potter, W. E., Hickman, D. R., and Mauersberger, K., "The Open-Source Neutral-Mass Spectrometer on Atmospheric Explorer-C, -D, and -E," *Radio Science*, Vol. 8, No. 4, 1973, pp. 271-276.

24. Arnold F., Krankowsky, D., Marien, K. H., and Joos, W., "A Mass Spectrometer Probe for Composition and Structure Analysis of the Middle Atmosphere Plasma and Neutral Gas," *Journal of Geophysics*, Vol. 44, No. 1-2,

1977, pp. 125-138.

25. Torr, D. G., and Torr, M. R., "Chemistry of the Thermosphere and Ionosphere," *Journal of Atmospheric and Terrestrial Physics*, Vol. 41, No. 7-8, 1979, pp. 797-839.

26. Philbrick, C. R., Schmidlin, F. J., Grossman, K. U., Lange, G., Offerman, D., Baker, K. D., Krankowsky, D., and von Zahn, U., "Density and Temperature Structure Over Northern Europe," *Journal of Atmospheric and Terrestrial Physics*, Vol. 47, No. 1-3, 1985, pp. 159-172.

27. Von Zahn U., Lubken, F. -J., and Putz, C., "BUGATTI Experiments: Mass Spectrometric Studies of Lower Thermosphere Eddy Mixing and Turbulence," *Journal of Geophysical Research*, Vol. 95, No. D6, 1990, pp. 7443-7465.

28. Hansen, W., private communication, The Center for Space Sciences, University of Texas at Dallas, Richardson, Texas, August, 1990.

29. Anon., "Ion Trap Mass Spectrometer", Finnigan MAT®, San Jose, CA, 1989.

30. Dawson, P. H., Hedman, J. W., and Whetten, N. R., "A Simple Mass Spectrometer," *The Review of Scientific Instruments*, Vol. 40, No. 11, 1969, pp. 1444-1450.

31. Dawson, P. H., and Lambert, C., "High Pressure Characteristics of the Quadrupole Ion Trap," *Journal of Vacuum Science Technology*, Vol. 12, No. 4, 1975, pp. 941-942.

32. Wojcik, R. M., Schilling, J. H., and Erwin, D. A., "Rarefied Flow Diagnostics Using Pulsed High-Current Electron Beams," AIAA Paper 90-1515, June, 1990.

33. Sabbagh, J., and Bonifazi, C., "Scientific Experiments on Board the TSS Satellite," Tethers in Space - Toward Flight, AIAA, Washington, DC, May, 1989, p. 409.

34. Hoffman, J. H., "Ion Composition Down to 130 km - From Atmospheric Explorer C to TSS2," Tethers in Space - Toward Flight, AIAA, Washington, DC, May, 1989, pp. 136-140.

35. Narcisi, R., Bailey, A., Federico, G., and Wlodyka, L., "Positive and Negative Ion Composition Measurements in the D- and E- Regions During the 26 February 1979 Solar Eclipse," *Journal of Atmospheric and Terrestrial Physics*, Vol. 45, No. 7, 1983, pp. 461-478.

36. Grossman, K. U., Frings, W. G., Offerman, D., Andre, L., Kopp, E., and Krankowsky, D., "Concentrations of H_2O and NO in the Mesosphere and the Lower Thermosphere at High Latitudes," *Journal of Atmospheric and Terrestrial Physics*, Vol. 47, No. 1-3, 1985, pp. 291-300.

37. Kopp, E., Andre, L., and Smith, L. G., "Positive Ion Composition and Derived Particle Heating in the Lower Auroral Ionosphere," *Journal of Atmospheric and Terrestrial Physics*, Vol. 47, No. 1-3, 1985, pp. 301-308.

38. Torkar, K. M., Urban, A., Bjordal, J., Lundblad, J. A., Soraas, F., Smith, L. G., Dumbs, A., Grandal, B., Ulwick, J. C., and Vancour, R. P., "Energy Deposition Rates by Charged Particles," *Journal of Atmospheric and Terrestrial Physics*, Vol. 47, No. 1-3, 1985, pp. 61-71.

39. Curtis, S. A., Hoegy, W. R., Brace, L. H., Maynard, N. C., Suguira, M., and

Winningham, J. D., "DE-2 Cusp Observations: Role of Plasma Instabilities in Topside Ionospheric Heating and Density Fluctuations," *Geophysical Research Letters*, Vol. 9, No. 9, 1982, pp. 997-1000.

40. Sojka, J. J., Schunk, R. W., Johnson, J. F. E., Waite, J. H., and Chappell, C. R., "Characteristics of Thermal and Suprathermal Ions Associated with the Dayside Plasma Trough as Measured by the Dynamics Explorer Retarding Ion Mass Spectrometer," *Journal of Geophysical Research*, Vol. 88, No. A10, 1983, pp. 7895-7911.

41. Koehbiel, J. P., Brace, L. H., Theis, R. F., Pincus, W. H., and Kaplan, R. B., "The Dynamics Explorer Langmuir Probe Instrument," *Space Science Instrumentation*, Vol. 5, 1981, pp. 493-500.

42. Baker, K. D., LaBelle, J., Pfaff, R. F., Howlett, L. C., Rao, N. B., Ulwick, J. C., and Kelley, M. C., "Absolute Electron Density Measurements in the Equatorial Ionosphere," *Journal of Atmospheric and Terrestrial Physics*, Vol. 47, No. 8-10, 1985, pp. 781-789.

43. Maynard, N. C., Bielicki, E. A., Burdick, H. G., "Instrumentation for Vector Field Measurements from DE-B," *Space Science Instrumentation*, Vol. 5, 1981, pp. 523-532.

44. Heelis, R. A., Hanson, W. B., Lippincott, C. R., Zuccaro, D. R., Harmon, L. H., Holt, B. J., Doherty, J. E., and Power, R. A., "The Ion Drift Meter for Dynamics Explorer-B," *Space Science Instrumentation*, Vol. 5, 1981, pp. 511-521.

45. McCoy, R.P., "Thermospheric Odd Nitrogen 1. NO, N(^{4}S), and O(^{3}P) Densities from Rocket Measurements of the NO δ and γ Bands and the O_2 Herzberg I Bands," *Journal of Geophysical Research*, Vol. 88, No. A4, 1983, pp. 3197-3205.

46. Hays, P. B., Carigan, G., Kennery, B. C., Shepherd, G. G., and Walker, J. C. G., "The Visible Airglow Experiment on Atmosphere Explorer," *Radio Science*, Vol. 8, No. 4, 1973, pp. 369-375.

47. Sharp, W. E., "Absolute Concentrations of O(^{3}P) in the lower Thermosphere," *Geophysical Research Letters*, Vol. 7, July, 1980, pp 485-488.

48. Sharp, W. E., "The Measurement of Atomic Oxygen in the Mesosphere and Lower Thermosphere," *Planetary Space Science*, Vol. 39, No. 4, 1991, pp 617-626.

49. Hedin, A. E., "MSIS Thermospheric Model," *Journal of Geophysical Research*, Vol. 92, No. A5, 1987, pp. 4649-4662.

50. Don Crouch, private communication, Martin-Marietta, Denver, Co., U.S.A., August, 1990.

51. Yee, J. H., and Abreu, V. J., "Visible Glow Induced by Spacecraft-Environment Interaction," *Geophysical Research Letters*, Vol. 10, No. 2, 1983, pp. 126-129.

52. Sugiura, M., Maynard, N. C., Farthing, W. H., Heppner, J. P., and Ledley, B. G., "Initial Results on the Correlation Between the Magnetic and Electric Fields Observed from the DE-2 Satellite in the Field-Aligned Current Regions,"

Geophysical Research Letters, Vol. 9, No. 9, 1982, pp. 985-988.

53. Rich, F. J., Cattell, C. A., Kelley, M. C., and Burke, W. J., "Simultaneous Observations of Auroral Zone Electrodynamics by Two Satellites: Evidence for Height Variations in the Topside Ionosphere," (and references therein), *Journal of Geophysical Research*, Vol. 86, No. A11, 1981, pp. 8929-8940.

54. Bythrow, P. F., Heelis, R. A., Hanson, W. B., and Power, R. A., "Simultaneous Observations of Field-Aligned Currents and Plasma Drift Velocities by Atmospheric Explorer C," *Journal of Geophysical Research*, Vol. 85, No. A1, 1980, pp. 151-159.

55. Acuna, M. H., Scearce, C. S., Seek, J. B., and Scheifele, J., "The Magsat Vector Magnetometer - A Precision Fluxgate Magnetometer for the Measurement of the Geomagnetic Field," NASA TM-79565, Oct., 1978.

56. Farthing, W. H., "The Magsat Scalar Magnetometer," *Johns Hopkins APL Technical Digest*, Vol. 1, No. 3, 1980, pp. 205-209.

57. Langel, R. A., Estes, R. H., Mead, G. D., Fabiano, E. B., and Lancaster, E. R., "Initial Geomagnetic Field Model from Magsat Vector Data," *Geophysical Research Letters*, Vol. 7, No. 10, 1980, pp. 793-796.

58. Webster, W. J., Taylor, P. T., Schnetzler, C. C., and Langel, R. A., "The Magnetic Field of the Earth: Performance Considerations for Space-Based Observing Systems," *IEEE Transactions on Geoscience and Remote Sensing*, GE-23, 1985, pp. 541-551.

59. Throckmorton, D. A., "Benchmark Aeroheating Data from the First Flights

of the Space Shuttle Orbiter," AIAA Paper 82-0003, Jan., 1982.

60. Leger, L. J., Visentine, J. T., Kuminecz, J. F., and Spiker, I. K., "STS-8 Atomic Oxygen Effect Experiment," AIAA Paper 85-0415, Jan., 1985.

61. Kinard, W., "Long Duration Exposure Facility (LDEF) Results," AIAA Paper 91-0096, Jan., 1991.

62. Peters, P. N., Sisk, R. C., and Gregory, J. C., "Velocity Distributions of Oxygen Atoms Incident on Spacecraft Surfaces," *Journal of Spacecraft and Rockets*, Vol. 25, No. 1, 1988, pp. 53-58.

63. Cross, J. B., and Blais, N. C., "High-Energy/Intensity CW Atomic Oxygen Beam Source," Rarefied Gas Dynamics: Space-Related Studies, (eds. Muntz, E. P., Weaver, D. P., and Campbell, D. H.), in *Progress in Astronautics and Aeronautics*, AIAA, Washington, DC, Vol. 116, 1989, pp. 143-155.

64. Arnoldy, R. L., and Winckler, J. R., "The Hot Plasma Environment and Floating Potentials of an Electron-Beam-Emitting Rocket in the Ionosphere," *Journal of Geophysical Research*, Vol. 86, No. A2, 1981, pp. 574-584.

65. Arnoldy, R. L., Pollock, C., and Winckler, J. R., "The Energization of Electrons and Ions by Electron Beams Injected in the Ionosphere," *Journal of Geophysical Research*, Vol. 90, No. A6, 1985, pp. 5197-5210.

66. Waterman, J., Wilhelm, K., Torkar, K. M., and Riedler, W., "Space Shuttle Charging or Beam-Plasma Discharge: What Can Electron Spectrometer Observations Contribute to Solving the Question?," *Journal of Geophysical Research*, Vol. 93, No. A5, 1988, pp. 4134-4140.

LIST OF FIGURES

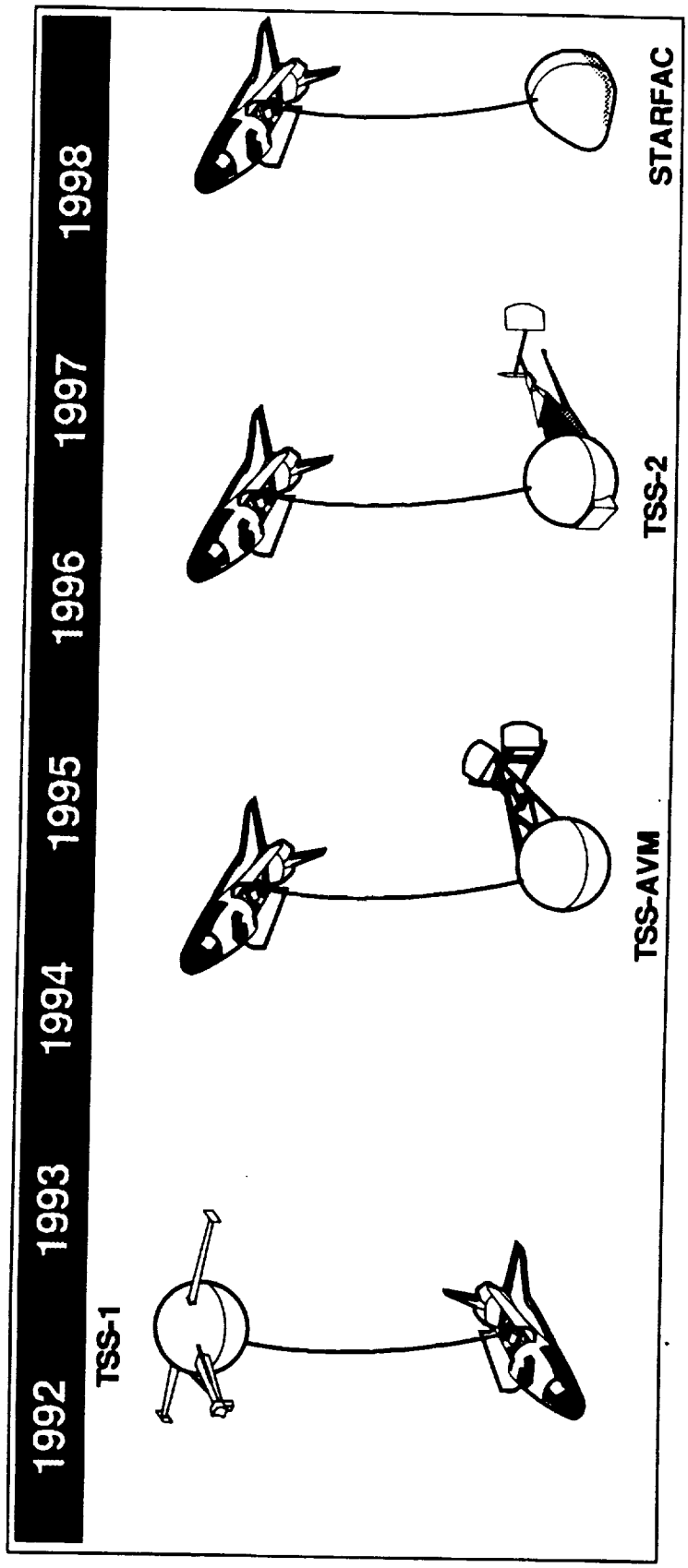

Fig. 1

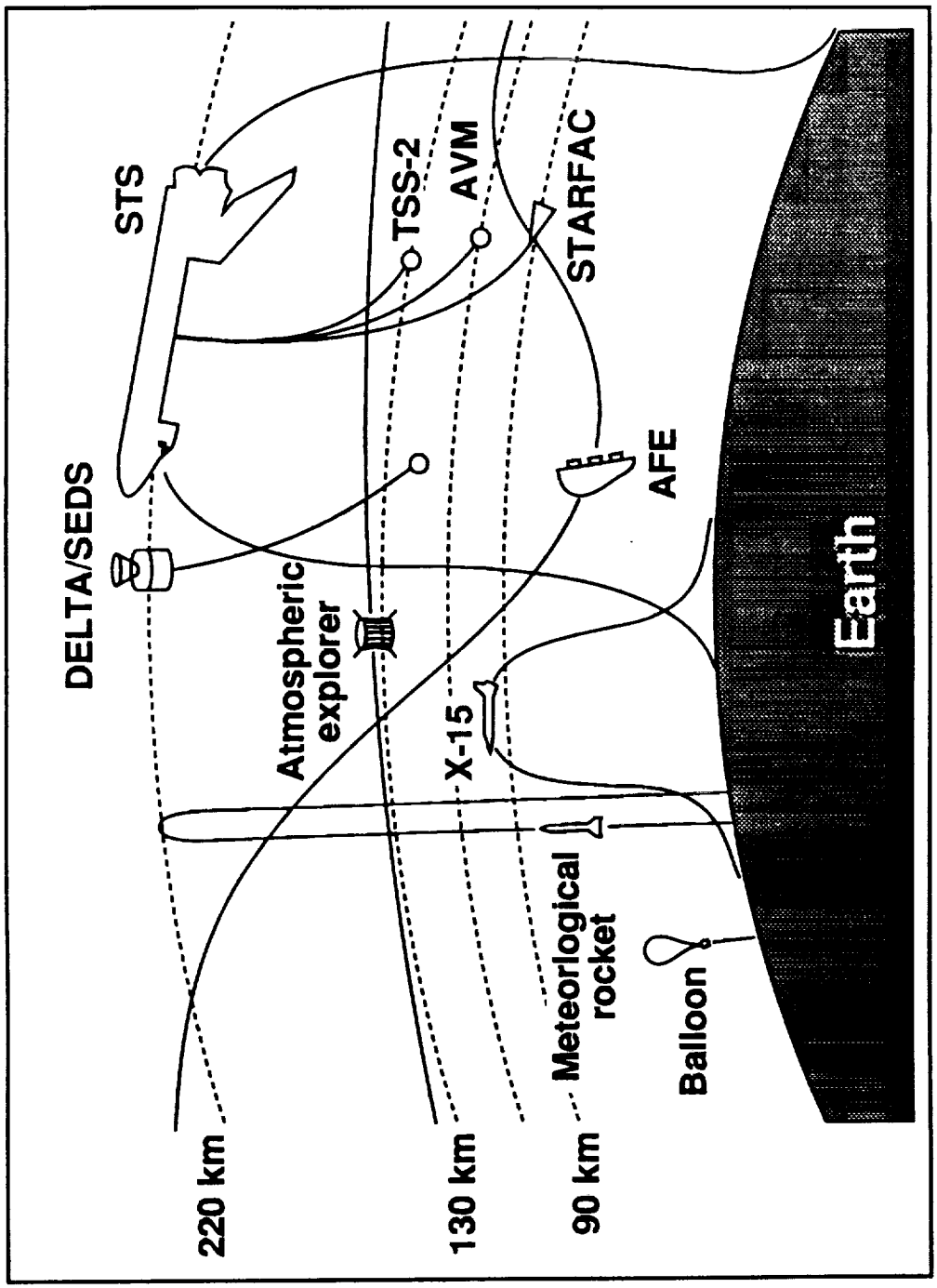
STS
TSS-2
AVM
STARFAC
DELTA/SEDS
Atmospheric explorer
AFE
X-15
Earth
Meteorlogical rocket
Balloon
220 km
130 km
90 km

Fig. 2

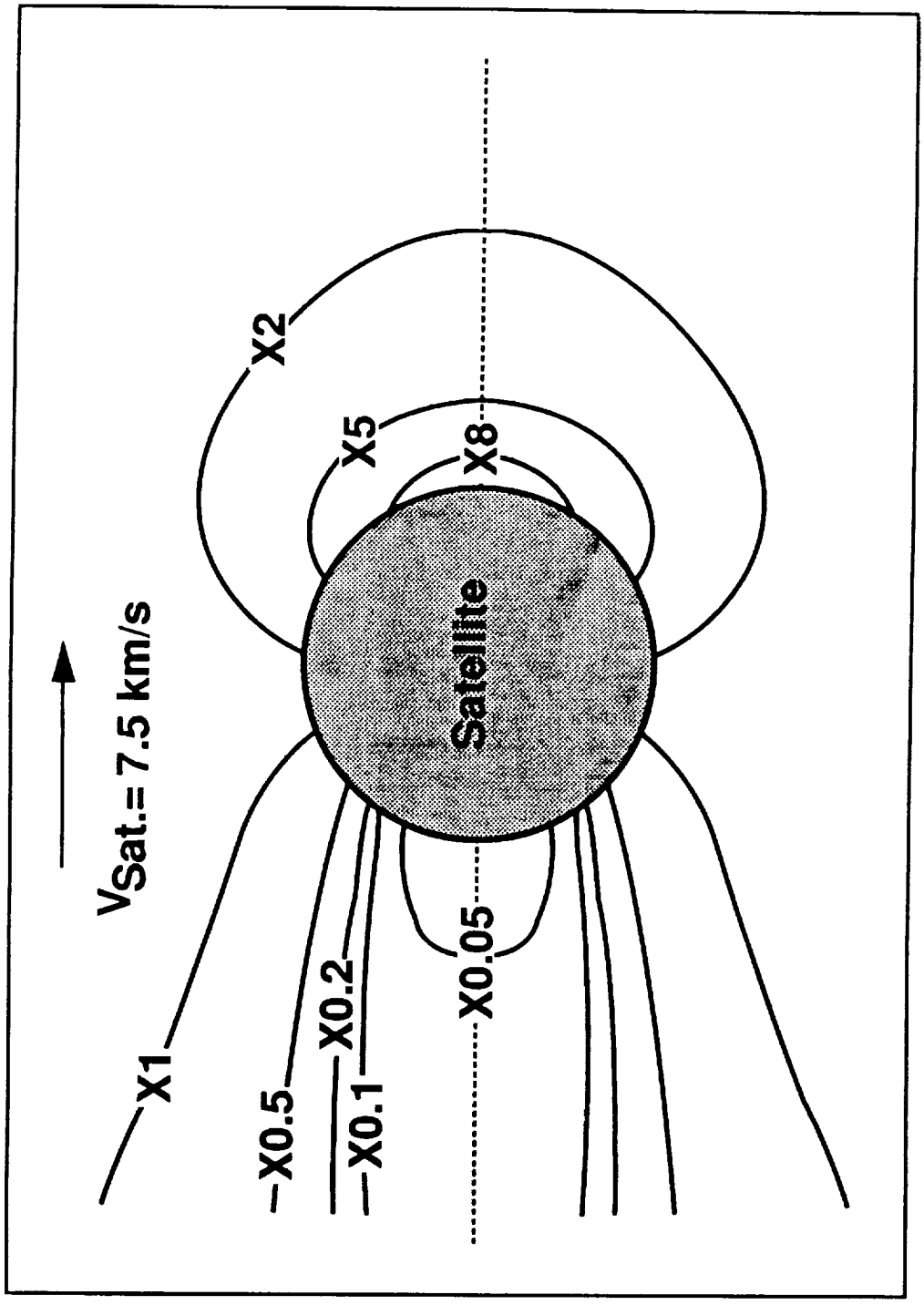

Fig. 3

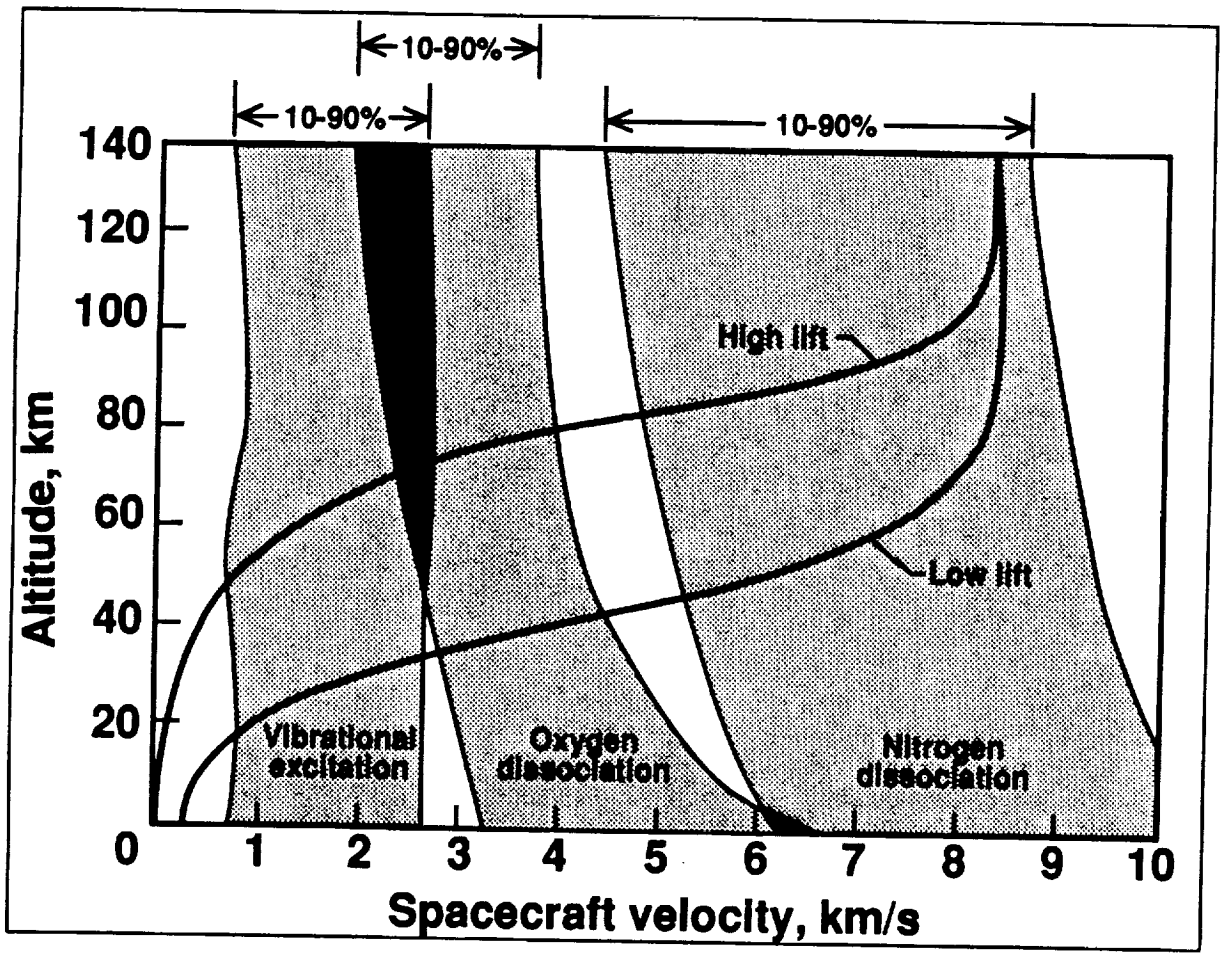
10-90%
10-90%
10-90%
140
120
100
80
60
40
20
0
Altitude, km
High lift
Low lift
Vibrational excitation
Oxygen dissociation
Nitrogen dissociation
1
2
3
4
5
6
7
8
9
10
Spacecraft velocity, km/s

Fig. 4

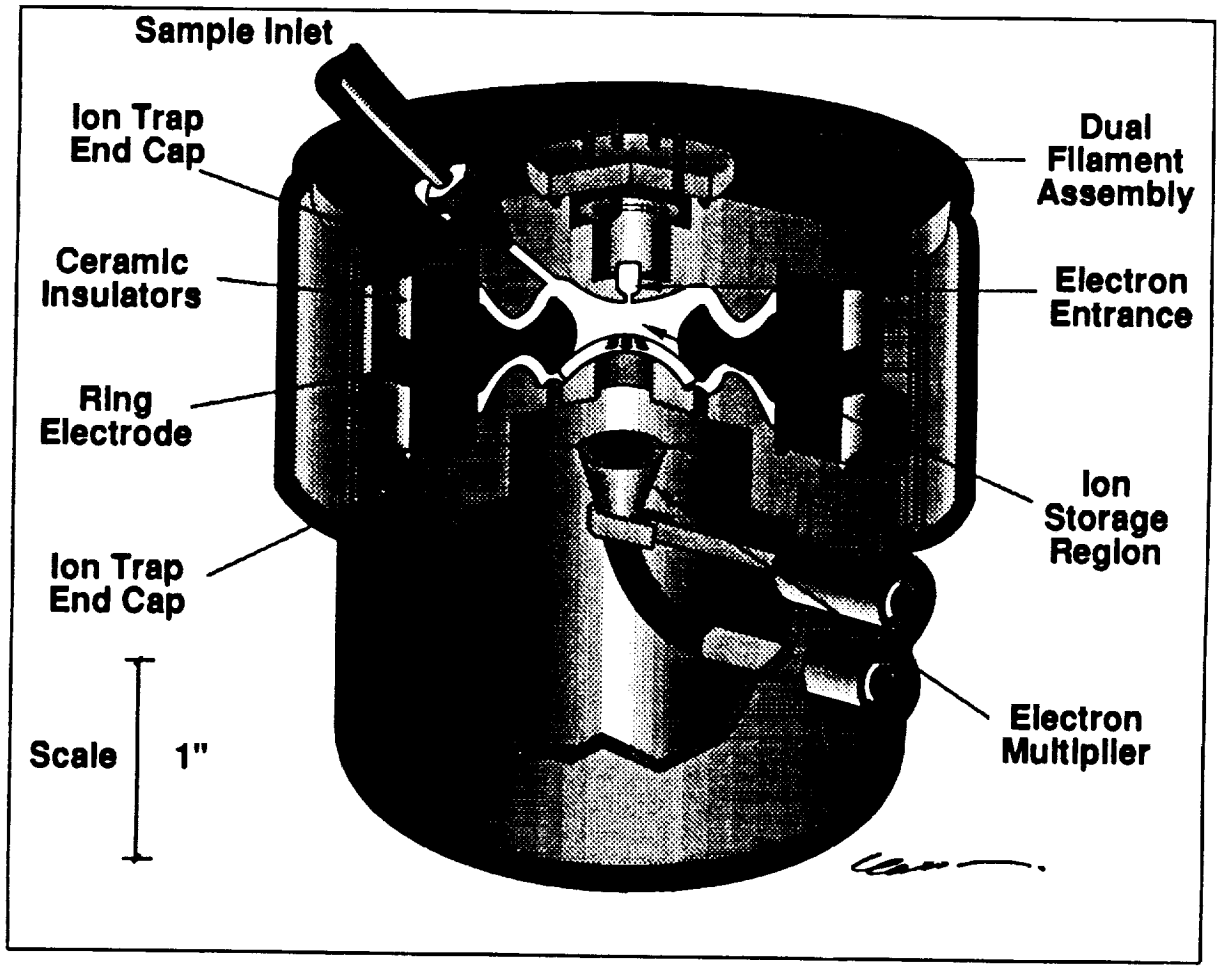
Sample Inlet
Ion Trap End Cap
Ceramic Insulators
Ring Electrode
Ion Trap End Cap
Scale 1"
Dual Filament Assembly
Electron Entrance
Ion Storage Region
Electron Multiplier

Fig. 5

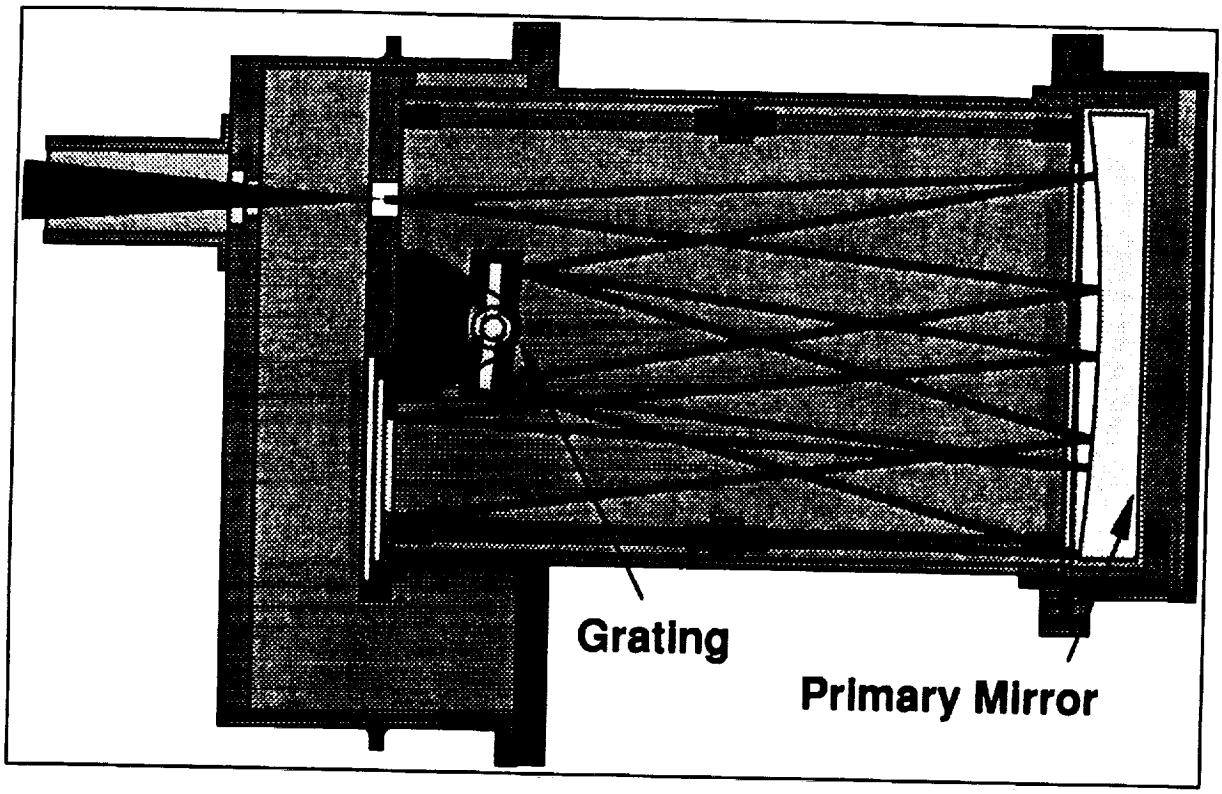

Fig. 6

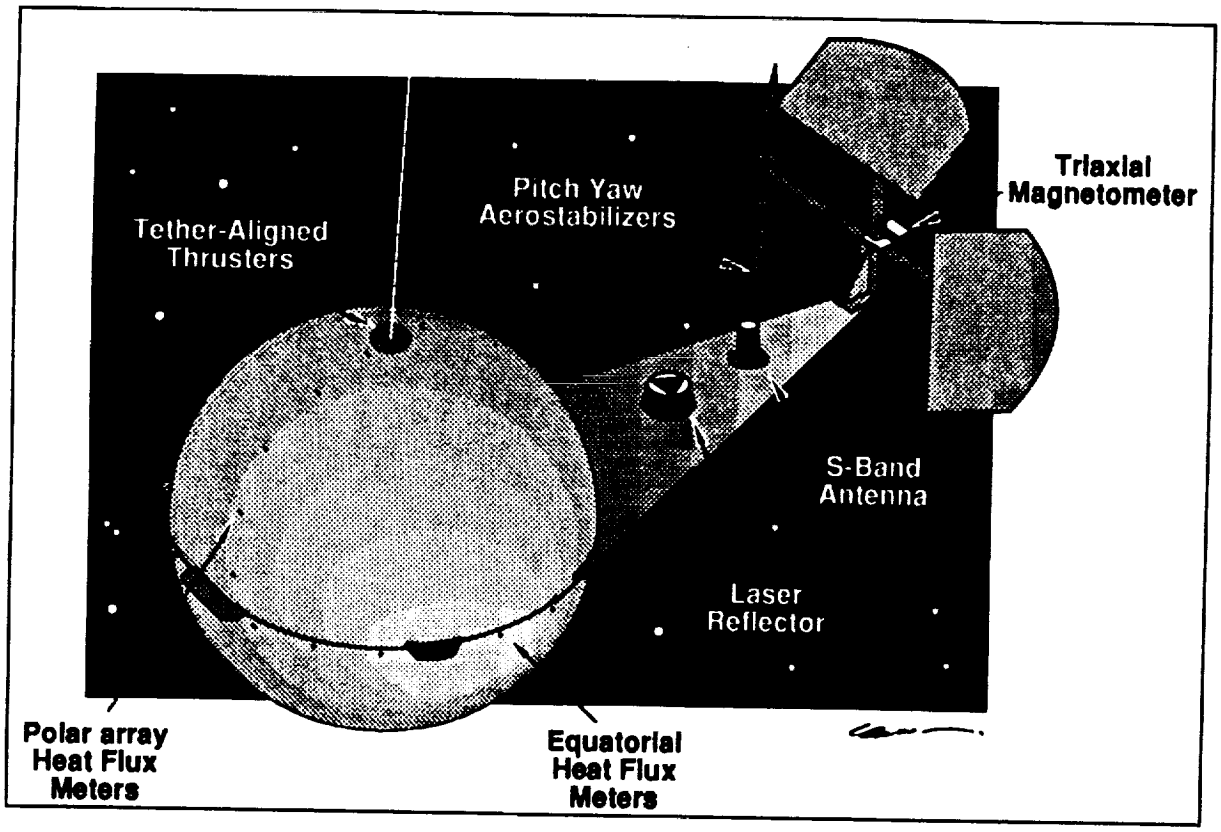
Tether-Aligned
Thrusters
Pitch Yaw
Aerostabilizers
Triaxial
Magnetometer
S-Band
Antenna
Laser
Reflector
Polar array
Heat Flux
Meters
Equatorial
Heat Flux
Meters

Fig. 7

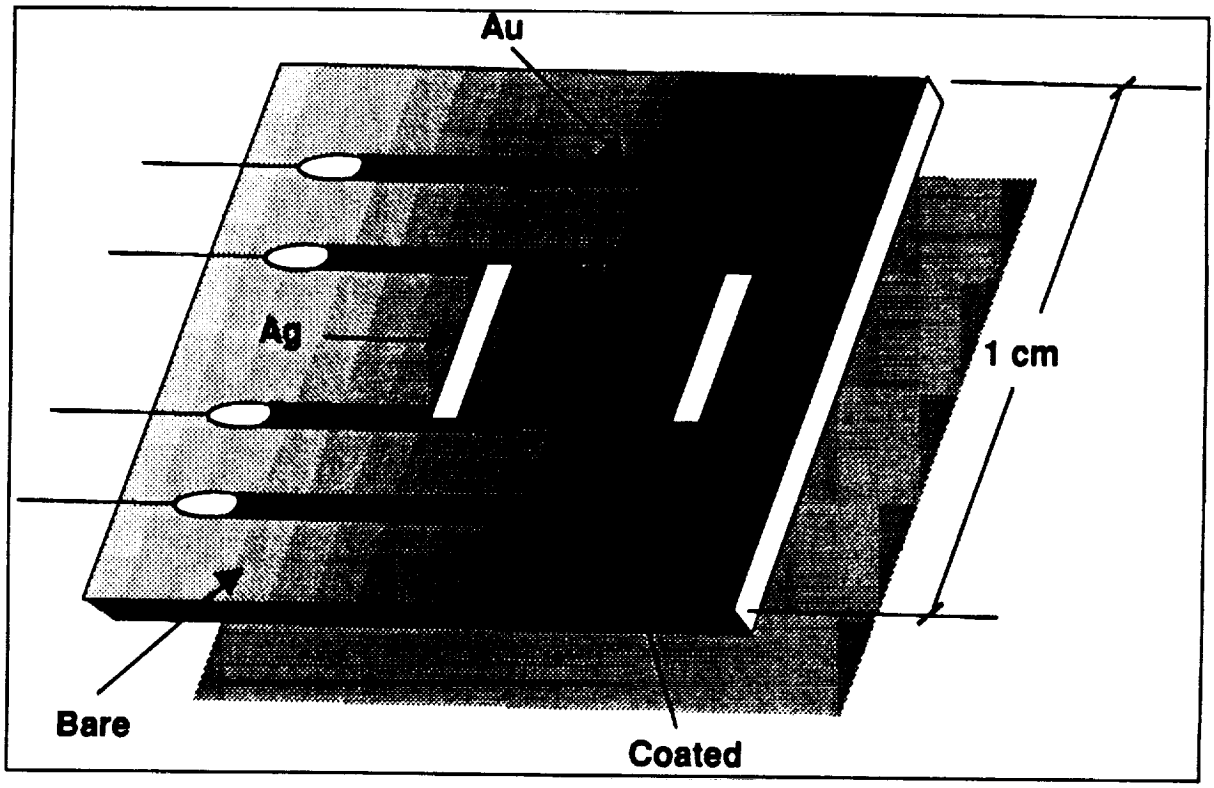

Fig. 8

REPORT DOCUMENTATION PAGE

Form Approved
OMB No. 0704-0188

1. AGENCY USE ONLY *(Leave blank)*

2. REPORT DATE
January 1992

3. REPORT TYPE AND DATES COVERED
Contractor Report

4. TITLE AND SUBTITLE
Instumentation for Hypersonic Aerodynamics Research with Tethered Satellites

5. FUNDING NUMBERS
C NAS1-18584
Task 73

967-30-30-01

6. AUTHOR(S)
Leonard T. Melfi, Jr.
Kenneth G. Brown, Jr.

7. PERFORMING ORGANIZATION NAME(S) AND ADDRESS(ES)
Old Dominion University Research Foundation
P.O. Box 6369
Norfolk, VA 23508-0369

8. PERFORMING ORGANIZATION REPORT NUMBER

9. SPONSORING / MONITORING AGENCY NAME(S) AND ADDRESS(ES)
National Aeronautics and Space Administration
Langley Research Center
Hampton, Virginia 23681-0001

10. SPONSORING / MONITORING AGENCY REPORT NUMBER
NASA CR-191435

11. SUPPLEMENTARY NOTES
Langley Technical Monitor - Kenneth H. Crumbly
Final Report

12a. DISTRIBUTION / AVAILABILITY STATEMENT
Unclassified - Unlimited
Subject Category 61

12b. DISTRIBUTION CODE

13. ABSTRACT *(Maximum 200 words)*

This report describes the work accomplished under Contract Number NAS1-18584 entitled "Master Agreement for Research in the Physical and Life Sciences." Task 73 entitled "Instrumentation for Hypersonic Aerodynamics Research with Tethered Satellites" with NASA LaRC. The work began on January 2, 1990, and extended through December 31, 1991. The first year's effort concentrated on shuttle borne tether satellite systems, measurement requirements, instrumentation assessment, aerothermodynamic instrumentation definition, and tether technology These aspects were studied in detail and are reported in a review article entitled "Downward Deployed Tethered Satellite Systems, Measurement Techniques, and Instrumentation: A Review" by Kenneth G. Brown, Jr. et. al, which has been accepted for publication in the May/June 1992 issue of the Journal of Spacecraft and Rockets. The second year's effort concentrated on the development of computer codes to analyze instrument data from NASA's SEDS mission. This mission is planned to fly in early 1993 and consists of an instrumented end-mass deployed with a tether from an orbiting second stage of a Delta rocket.

14. SUBJECT TERMS
Tether Satellites, Instrumentation

15. NUMBER OF PAGES
109

16. PRICE CODE

17. SECURITY CLASSIFICATION OF REPORT	18. SECURITY CLASSIFICATION OF THIS PAGE	19. SECURITY CLASSIFICATION OF ABSTRACT	20. LIMITATION OF ABSTRACT
Unclassified	Unclassified	Unclassified	